Aero-Propulsive Modeling for a Subscale Tiltrotor eVTOL Aircraft from Wind-Tunnel and Flight-Test Data

Dr. Benjamin M. Simmons

Vehicle Dynamics and Control Branch

NASA Langley Research Center

Dave Ward Memorial Lecture

ACGSC Meeting #137, 7–9 October 2026

Contents

- Research motivation/challenges
- RAVEN-SWFT vehicle
- Static wind-tunnel testing
- Dynamic wind-tunnel testing
- Flight-test system identification
- Concluding remarks
- Questions/discussion

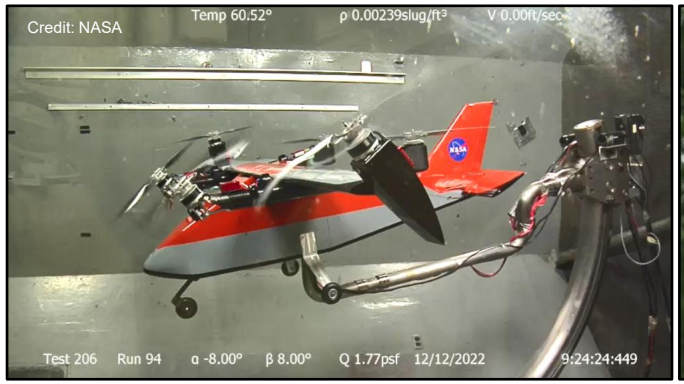
Software:
- MATLAB®/Simulink®
- SIDPAC
- Design-Expert®





Research Overview

- **Topic:** Electric vertical takeoff and landing (eVTOL) aircraft system ID
- Development of nonlinear aircraft mathematical models
- Flight dynamics simulations
- Models identified using data from:



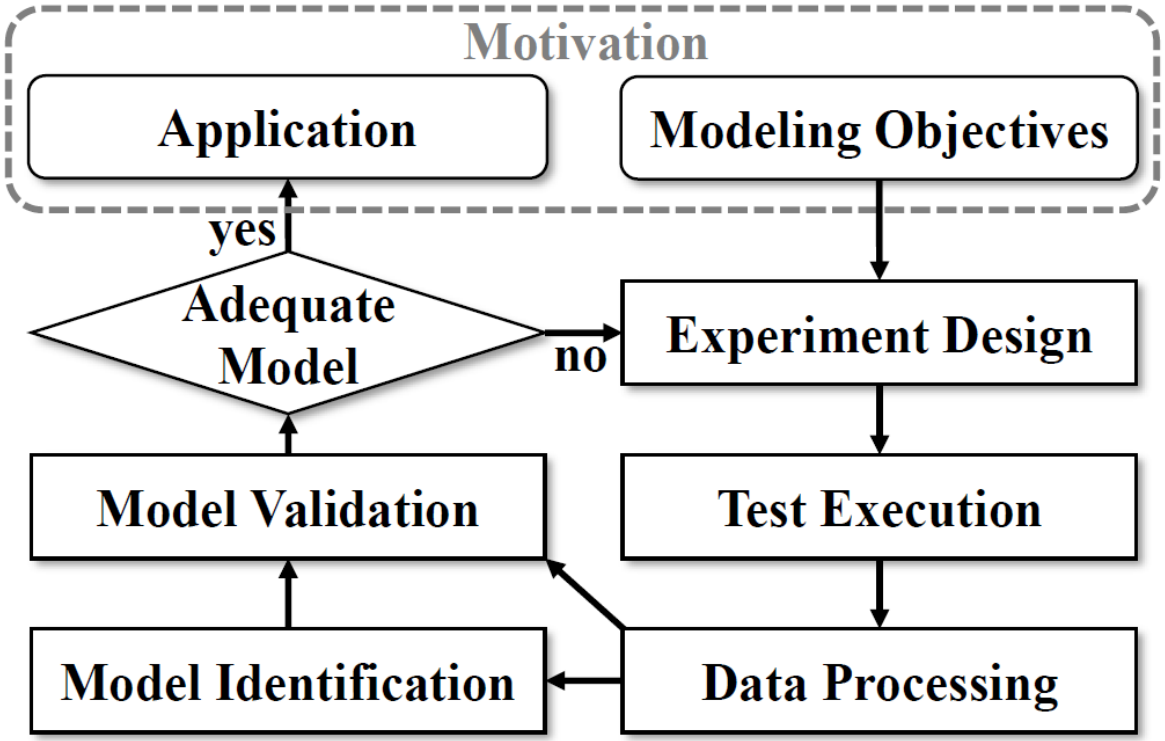
Wind-tunnel testing.



Flight testing.



System Identification



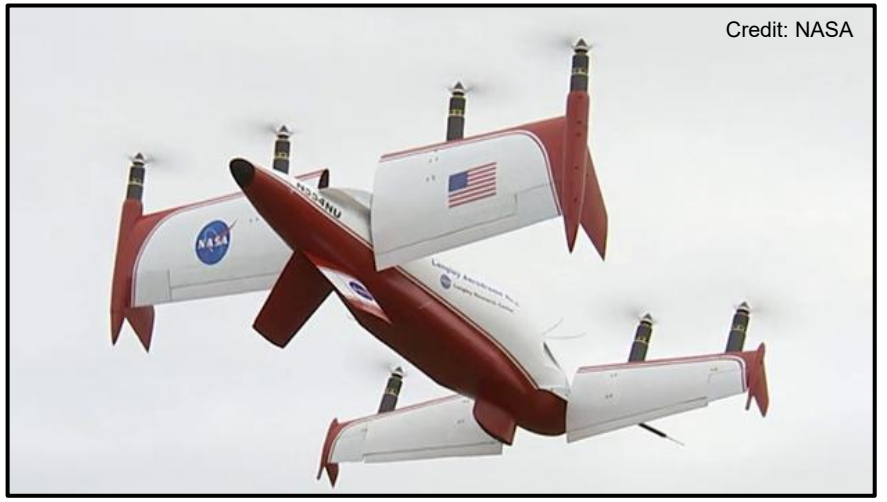
General system identification process.

Research Motivation

- Recent technology advancements enabling practical eVTOL aircraft
- Future Advanced Air Mobility (AAM) transportation system
- Multidisciplinary need for flight simulations driven by high-fidelity aero-propulsive models
- eVTOL vehicles are a new class of aircraft with numerous challenges
- Conventional methods fail to efficiently characterize eVTOL aircraft
- New eVTOL aircraft testing and modeling strategies are required



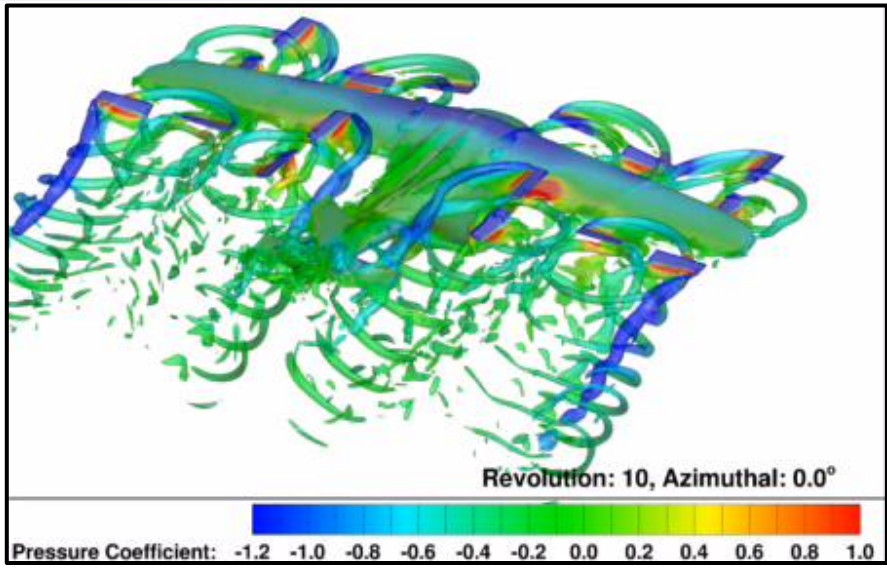
NASA GL-10 aircraft



NASA LA-8 aircraft

eVTOL Aircraft Modeling Challenges

- Many control surfaces and propulsors
- Significant propulsion-airframe interactions
- Integrated aero-propulsive modeling
- High incidence angle proprotor aerodynamics
- Vehicle instability
- Large flight envelopes to characterize
- Rapidly changing transition aerodynamics
- Characteristics of multiple aircraft types
- Many different configurations



eVTOL aircraft CFD simulation.
Credit: Brian G. Allan (NASA Langley)

1,200+ known eVTOL aircraft concepts!
Reference: https://evtol.news/aircraft

eVTOL vehicle configurations exhibit highly complex, nonlinear aerodynamics

Advanced Air Mobility (AAM)



RAVEN-SWFT

Research **A**ircraft for e**V**TOL **E**nabling Tech**N**ologies (RAVEN)[1]
Subscale **W**ind-Tunnel and **F**light **T**est (SWFT)[2] Vehicle

- Subscale tiltrotor eVTOL aircraft configuration
- Wind-tunnel and flight-test research
- Similar scale to LA-8 with expanded utility
- 24 independent control effectors
  - Six proprotor speeds $(n_1, n_2, \ldots, n_6)$
  - Six collective angles $(\delta_{c_1}, \delta_{c_2}, \ldots, \delta_{c_6})$
  - Four nacelle tilt angles $(\delta_{t_1}, \delta_{t_2}, \delta_{t_3}, \delta_{t_4})$
  - Six flaperons $(\delta_{f_1}, \delta_{f_2}, \ldots \delta_{f_6})$
  - Stabilator (δ_s) and Rudder (δ_r)
- 38 lb, 5.7 ft wingspan, 19.5 in diam. proprotors
- 28.6% scale version of a 1000-lb-class vehicle
- Built for modeling and controls research
- Publishable geometry, data, and methods

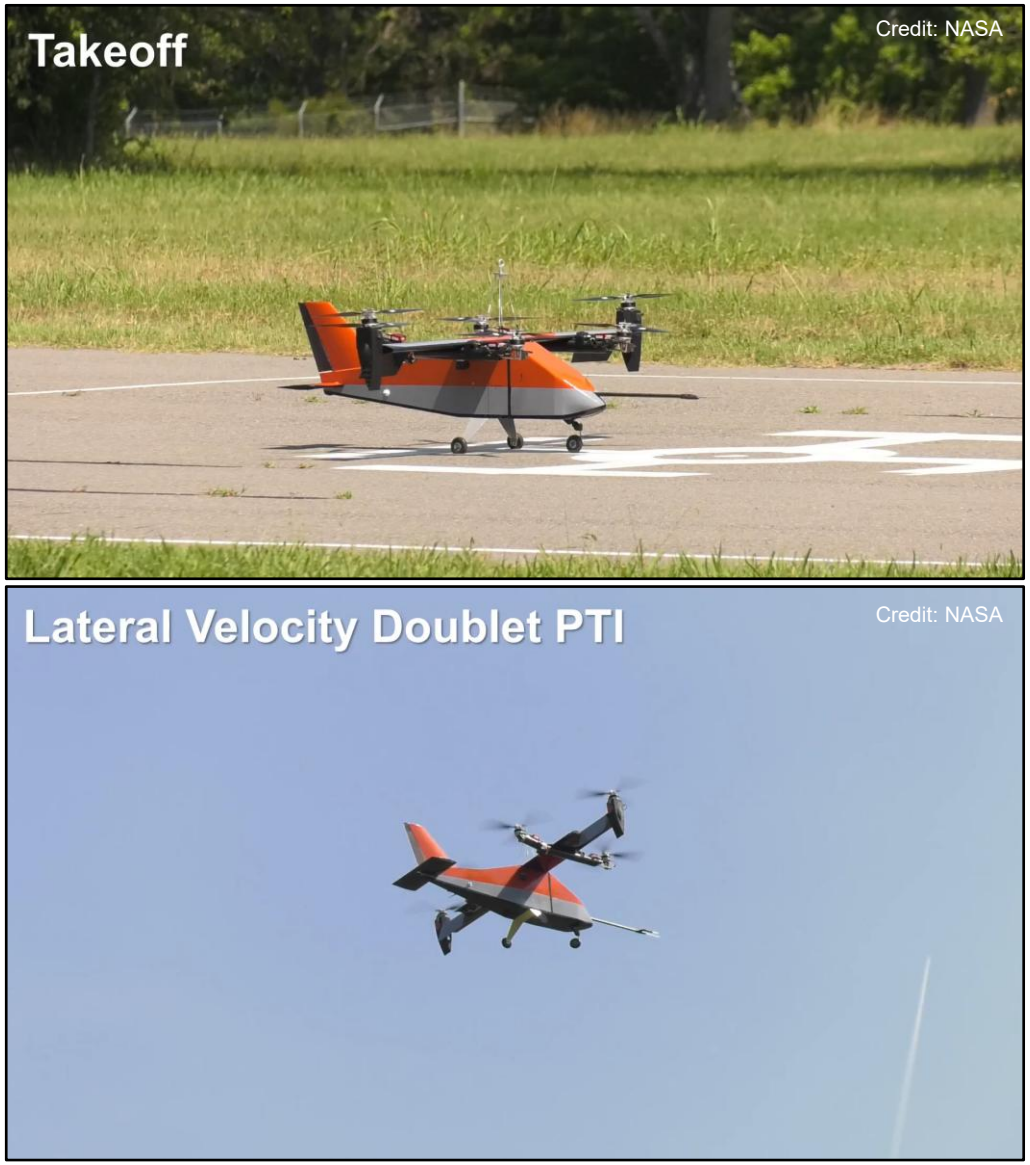




1. https://www.nasa.gov/raven/
2. Geuther, S. C., Simmons, B. M., and Ackerman, K. A., "Overview of the Subscale RAVEN Flight Controls and Modeling Testbed," *VFS Annual Forum*, May 2024.

RAVEN-SWFT Development and Testing

- Baseline wind-tunnel testing
  - Isolated proprotor test
  - Static full-airframe test
  - Dynamic 3DOF free-motion test
- Custom unified flight control algorithm
  - Model-based control design approach
  - Integrated using MathWorks® UAV Toolbox
- Ongoing flight-test envelope expansion
  - Flight control algorithm evaluation
  - System identification



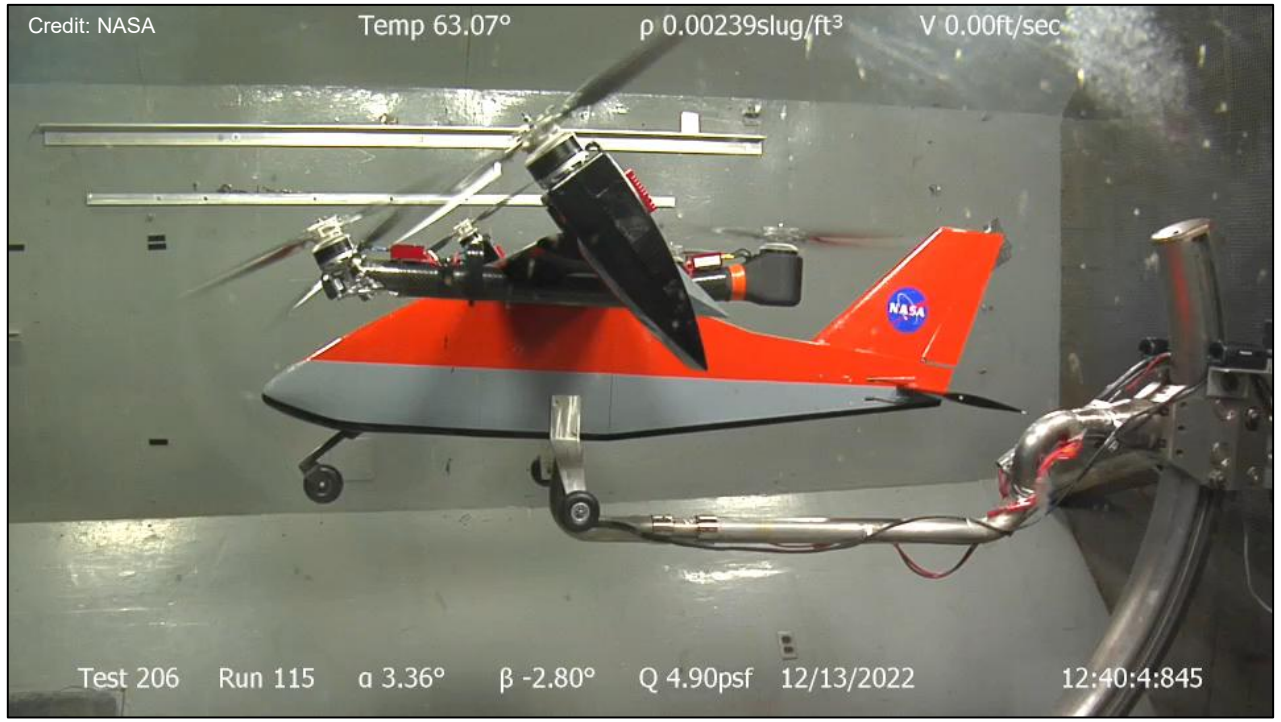
RAVEN-SWFT flight testing.

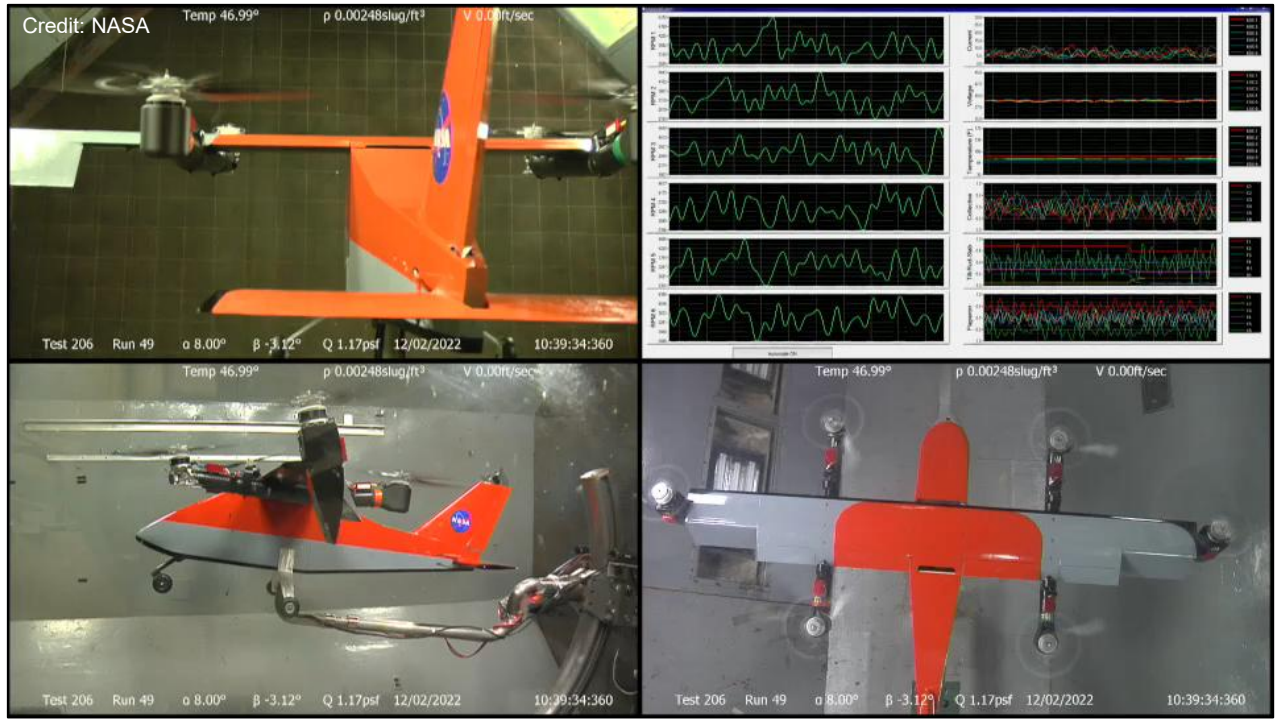
1. Simmons, B. M., Ackerman, K. A., Asper, G. D., Gray, M. N., Snyder, S. M., Axten, R. M., Geuther, S. C., and Chan, R., "Subscale Tiltrotor eVTOL Aircraft Dynamic Modeling and Flight Control Software Development," *VFS Annual Forum*, May 2025.

Static Wind-Tunnel Testing

Simmons, B. M., and Busan, R. C., “Statistical Wind-Tunnel Experimentation Advancements for eVTOL Aircraft Aero-Propulsive Model Development,” *AIAA SciTech Forum*, January 2024.

RAVEN-SWFT Powered-Airframe Testing



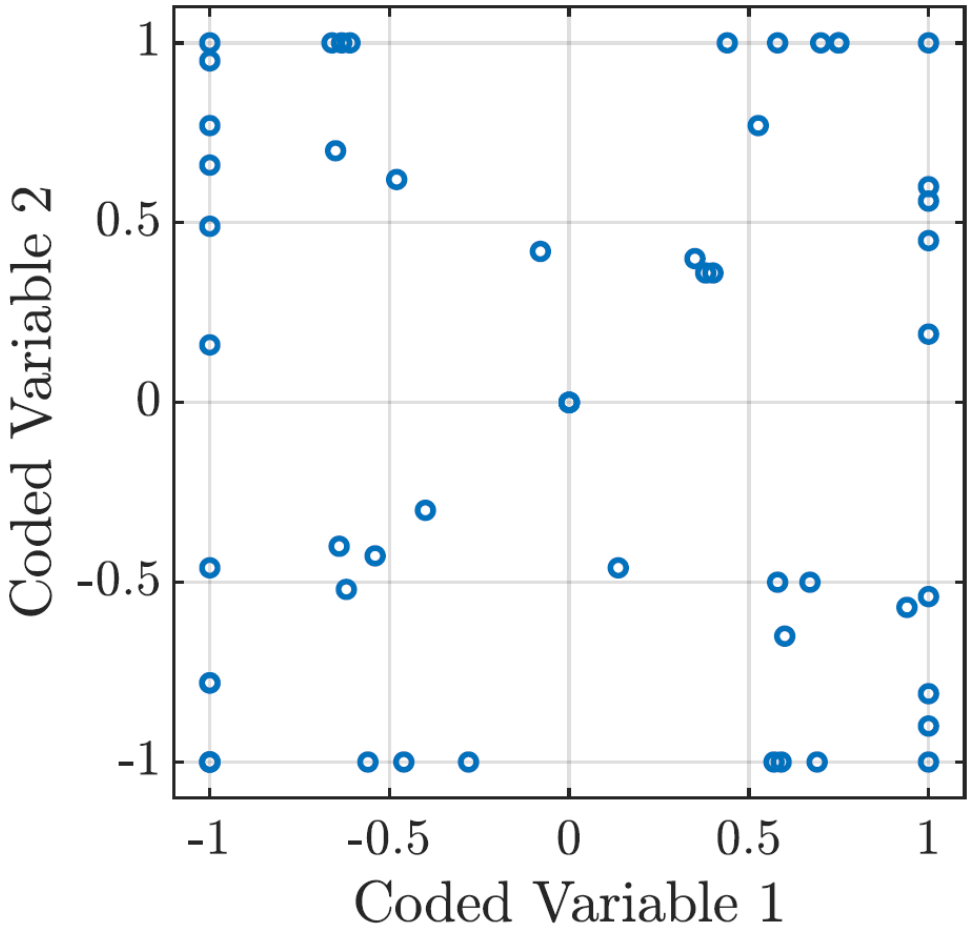


Static DOE/RSM testing (x20 speed). **Hybrid PTI/DOE/RSM testing (x1 speed).**

1. Simmons, B. M., "Evaluation of Response Surface Experiment Designs for Distributed Propulsion Aircraft Aero-Propulsive Modeling," *AIAA SciTech Forum*, January 2023.
2. Simmons, B. M., Morelli, E. A., Busan, R. C., Hatke, D. B., and O'Neal, A. W., "Aero-Propulsive Modeling for eVTOL Aircraft Using Wind Tunnel Testing with Multisine Inputs," *AIAA AVIATION Forum*, June 2022.
3. Simmons, B. M., and Busan, R. C., "Statistical Wind-Tunnel Experimentation Advancements for eVTOL Aircraft Aero-Propulsive Model Development," *AIAA SciTech Forum*, January 2024.

Transition Trim Envelope Determination

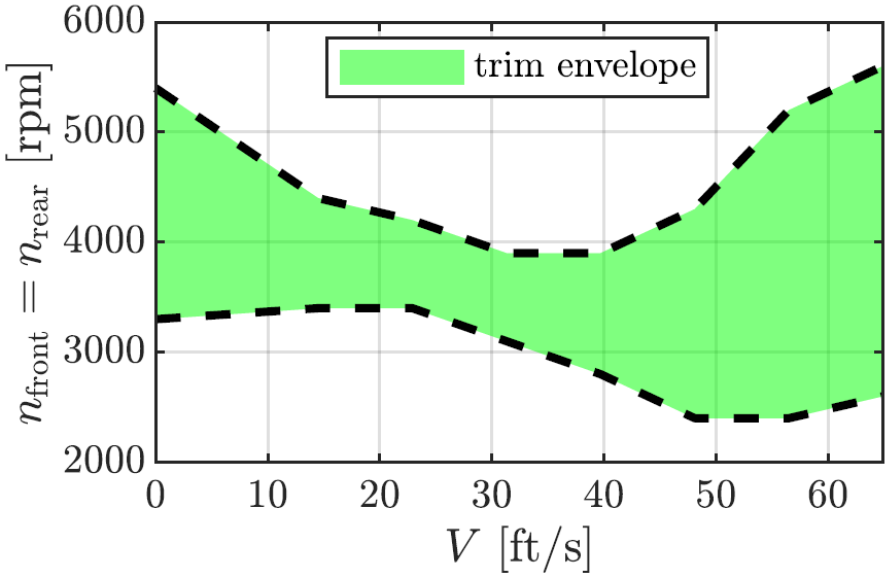
- Proper design space limits are important for transition characterization
- Specifying boundaries around the trim envelope is an effective approach
- New trim approach using DOE/RSM
  - Efficient, accurate, and mostly automated
  - Testing with a reduced number of factors
  - Level, unaccelerated transition envelope
  - Results inform subsequent aero-propulsive characterization experiments
- 8 dynamic pressure, $\bar{q}$, settings (low → high)
- Frugal design strategy (56 points per $\bar{q}$)
- 7 factor I-optimal response surface design



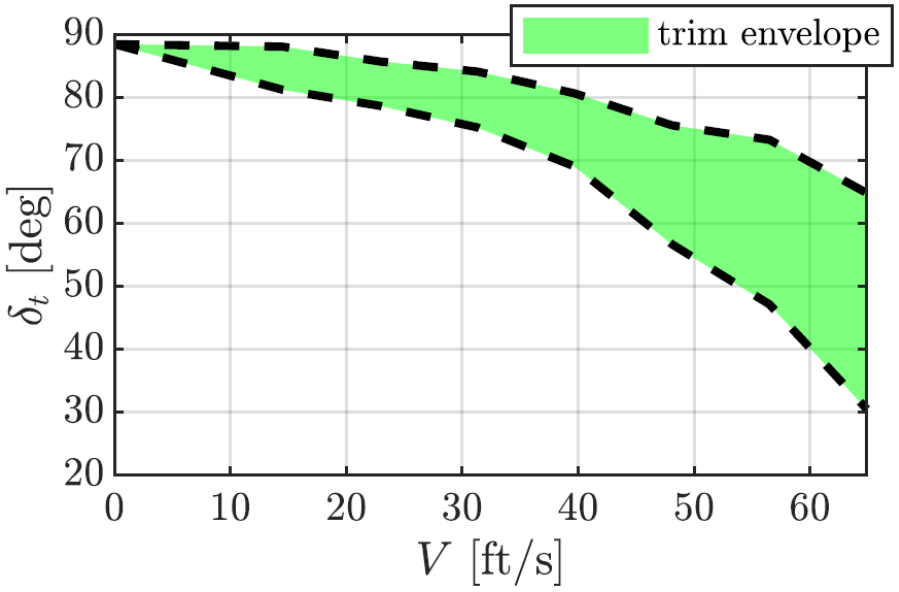
2D slice of the 7-factor trim experiment design in coded units.

Experimentally-Determined Trim Envelope

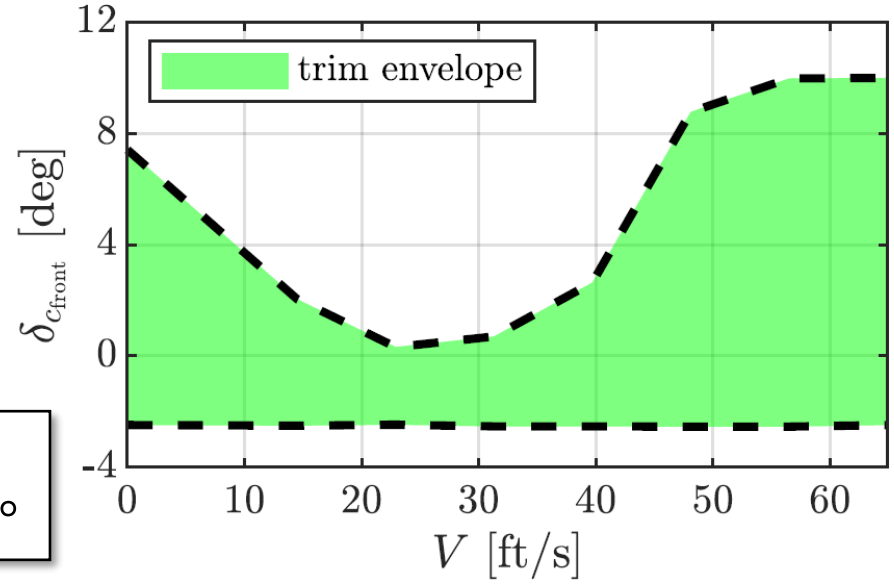
Proprotor rotational speed



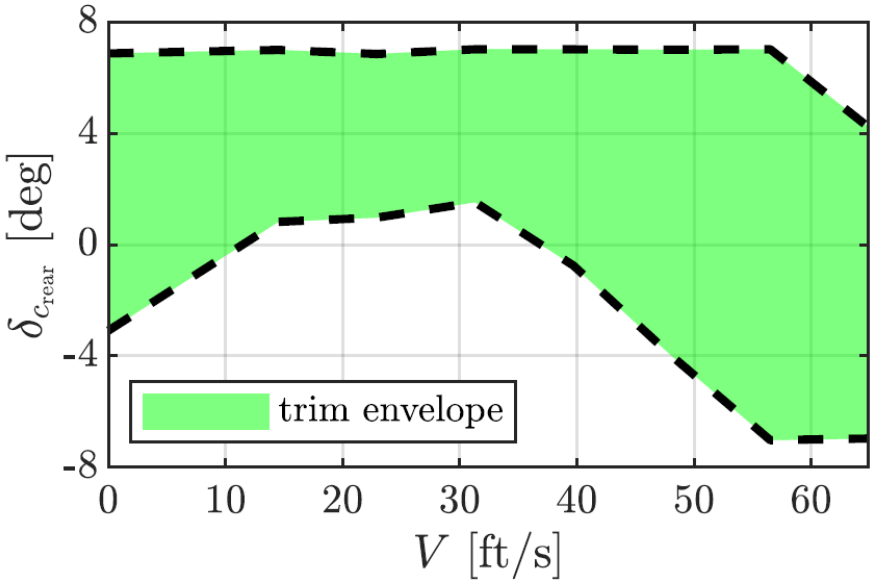
Nacelle Tilt Angle



Front Collective Angle



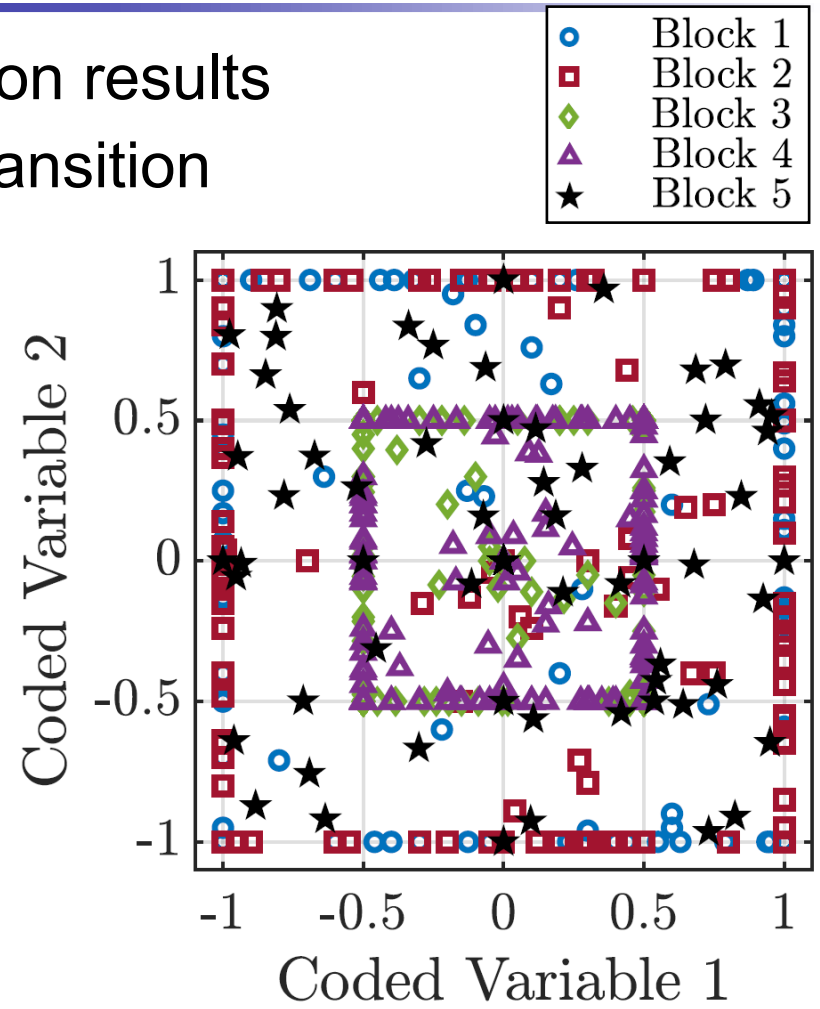
Rear Collective Angle



$\alpha = \beta = 0°$
$\delta_s = \delta_r = 0°$

Powered-Airframe Characterization

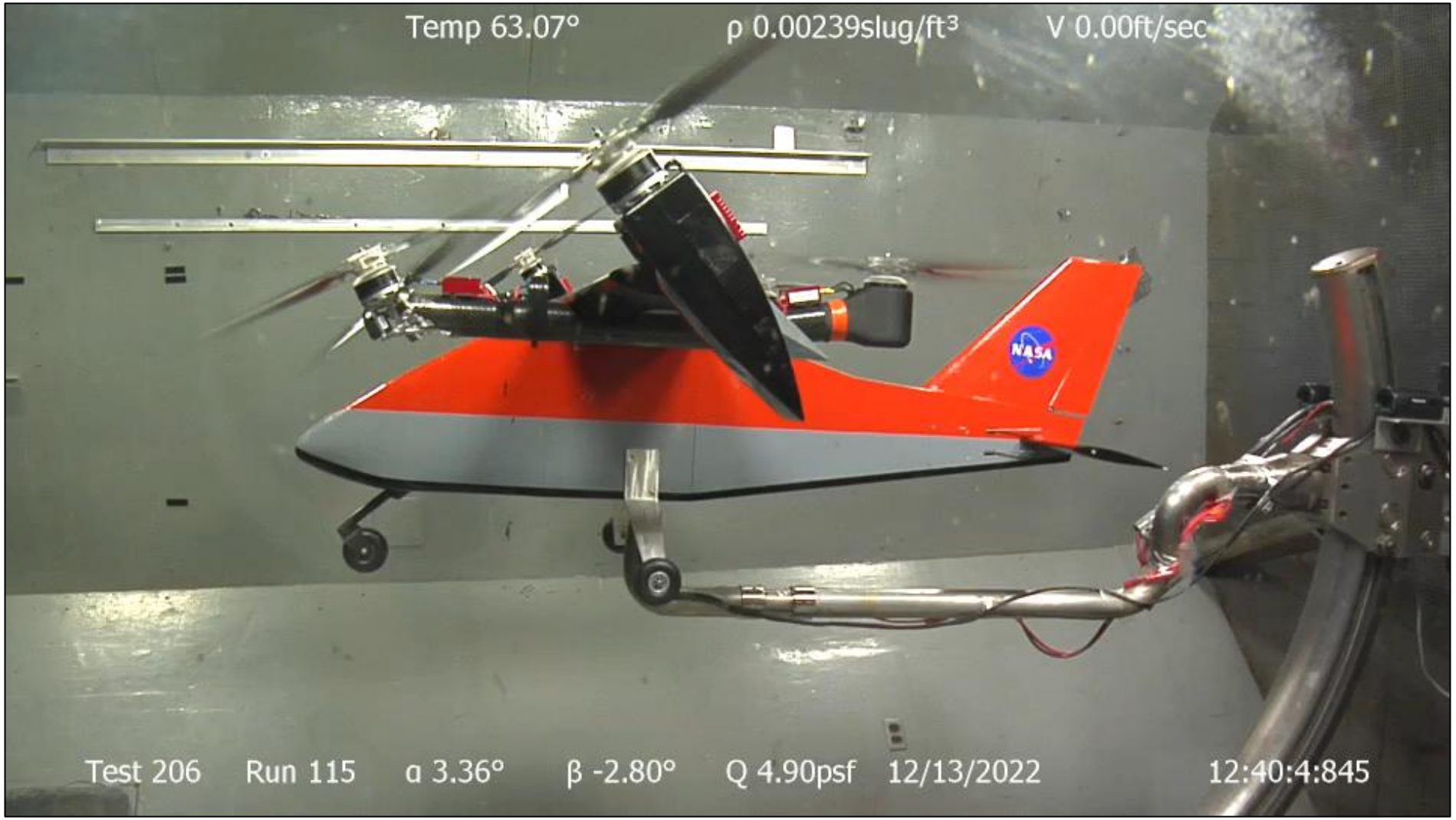
- Informed by the transition trim envelope determination results
- Powered-airframe testing from hover through mid-transition
- Eight dynamic pressure, $\bar{q}$, settings
- 26 independent test factors at each $\bar{q}$ setting
  - Angle of attack (α)
  - Angle of sideslip (β)
  - Motor speed commands ($\eta_{m_1}, \eta_{m_2}, \ldots, \eta_{m_6}$)
  - Collective pitch angles ($\delta_{c_1}, \delta_{c_2}, \ldots, \delta_{c_6}$)
  - Nacelle tilt angles ($\delta_{t_1}, \delta_{t_2}, \delta_{t_3}, \delta_{t_4}$)
  - Flaperon deflection angles ($\delta_{f_1}, \delta_{f_2}, \ldots \delta_{f_6}$)
  - Stabilator deflection angle (δ_s)
  - Rudder deflection angle (δ_r)
- Nested I-optimal design[1,2] (984 points per $\bar{q}$)



2D slice of the 26-factor experiment design in coded units.

1. Simmons, B. M., "Evaluation of Response Surface Experiment Designs for Distributed Propulsion Aircraft Aero-Propulsive Modeling," *AIAA SciTech Forum*, AIAA Paper 2023-2251, January 2023.
2. Simmons, B. M., and Busan, R. C., "Statistical Wind-Tunnel Experimentation Advancements for eVTOL Aircraft Aero-Propulsive Model Development," *AIAA SciTech Forum*, January 2024.

RAVEN-SWFT Wind-Tunnel Testing Video



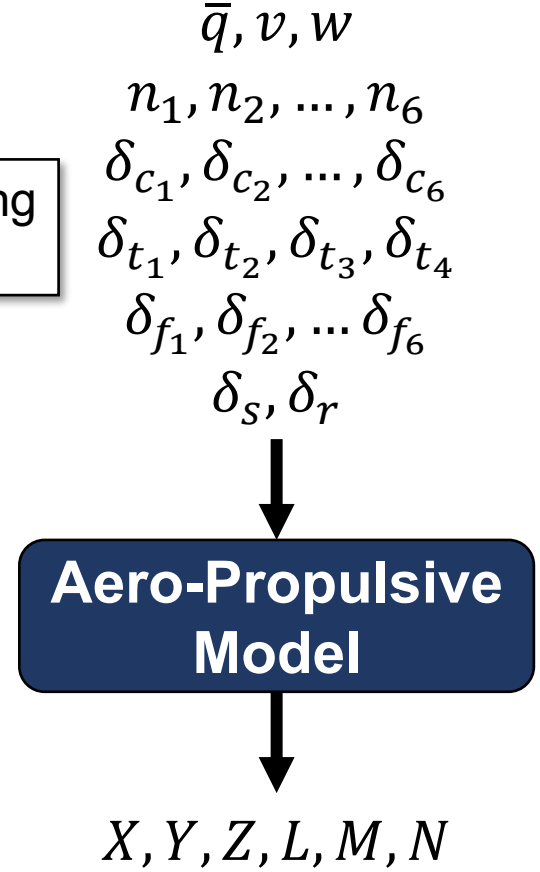
Static RAVEN-SWFT DOE/RSM wind-tunnel testing (x20 speed).

Model Identification Approach

- Aero-propulsive modeling framework tailored to eVTOL aircraft[1]
- Flight condition variable: dynamic pressure $\bar{q}$ (or freestream velocity V)
- Explanatory variables:
  - Body-axis velocity components (v, w)
  - Proprotor rotational speeds $(n_1, n_2, \dots, n_6)$
  - Control deflection angles $(\delta_{c_1}, \delta_{c_2}, \dots, \delta_{c_6}, \delta_{t_1}, \delta_{t_2}, \delta_{t_3}, \delta_{t_4}, \delta_{f_1}, \delta_{f_2}, \dots \delta_{f_6}, \delta_s, \delta_r)$

u effects are captured by models being developed at multiple $\bar{q}$ settings

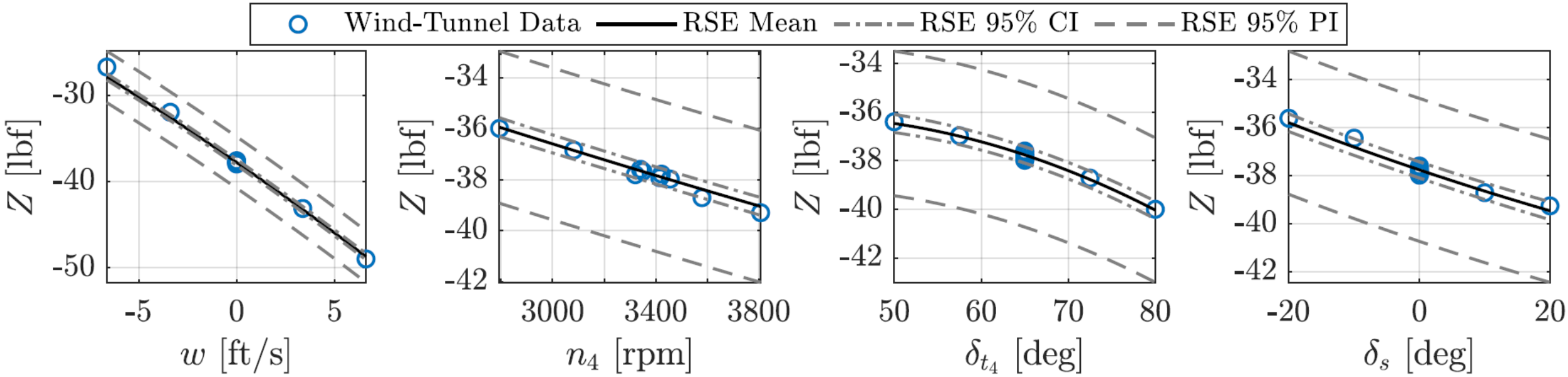
- Response variables:
  - Dimensional body-axis aero-propulsive forces (X, Y, Z)
  - Dimensional body-axis aero-propulsive moments (L, M, N)
- Nonlinear response surface equations (RSEs) developed at each $\bar{q}$
  - Model structure determination: stepwise regression[2]
  - Parameter estimation: ordinary least-squares regression[2]
- Continuous transition model formed by interpolating between RSEs



1. Simmons, B. M., and Murphy, P. C., "Aero-Propulsive Modeling for Tilt-Wing, Distributed Propulsion Aircraft Using Wind Tunnel Data," *Journal of Aircraft*, Vol. 59, No. 5, 2022, pp. 1162–1178.
2. Morelli, E. A., and Klein, V., Aircraft System Identification: Theory and Practice, 2nd ed., Sunflyte Enterprises, Williamsburg, VA, 2016.

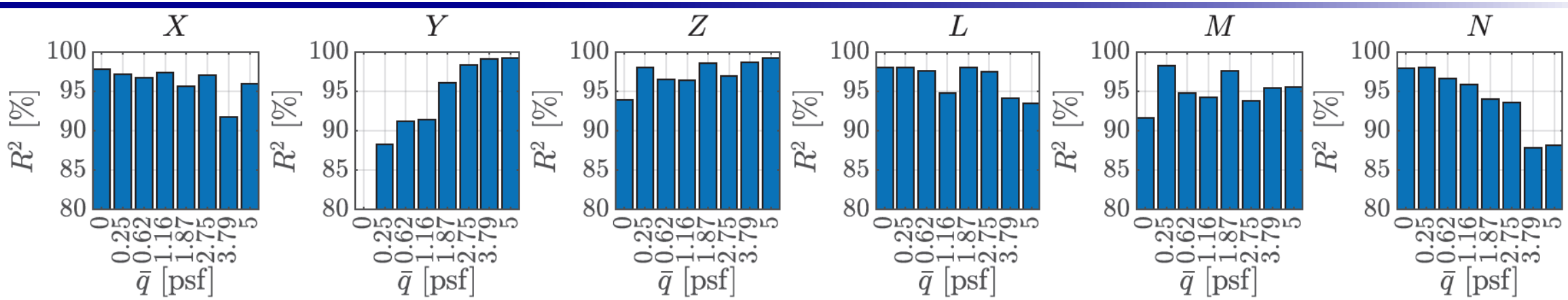
Sample Local Modeling Results

- RSE at $\bar{q}$ = 2.75 lbf/ft^2 compared to axial and center wind-tunnel data
- RSE predictions show good agreement with measured data
- Data are within the 95% prediction interval (PI)
- Similar results observed for other response variables and $\bar{q}$ settings



Model and wind-tunnel data comparison for explanatory variable sweeps ($\bar{q}$ = 2.75 lbf/ft^2).

Sample Global Modeling Results

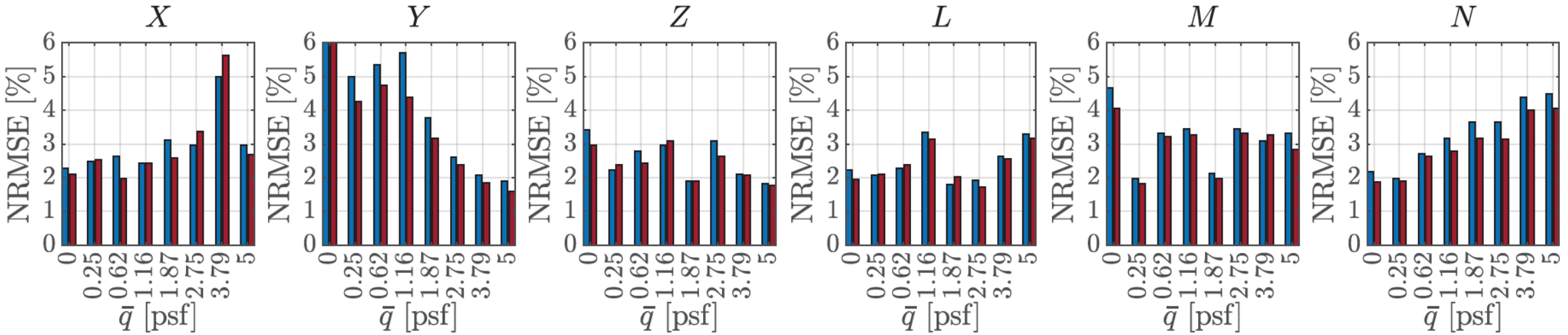


Coefficient of determination, R^2, for each local model.

$$R^2 = \frac{\hat{\boldsymbol{y}}^T \boldsymbol{z} - N\bar{z}^2}{\boldsymbol{z}^T \boldsymbol{z} - N\bar{z}^2}$$

Modeling Data Validation Data

$$\text{NRMSE} = 100 \times \frac{1}{\text{range}(\boldsymbol{z}_m)} \sqrt{\frac{(\boldsymbol{z} - \hat{\boldsymbol{y}})^T (\boldsymbol{z} - \hat{\boldsymbol{y}})}{N}}$$



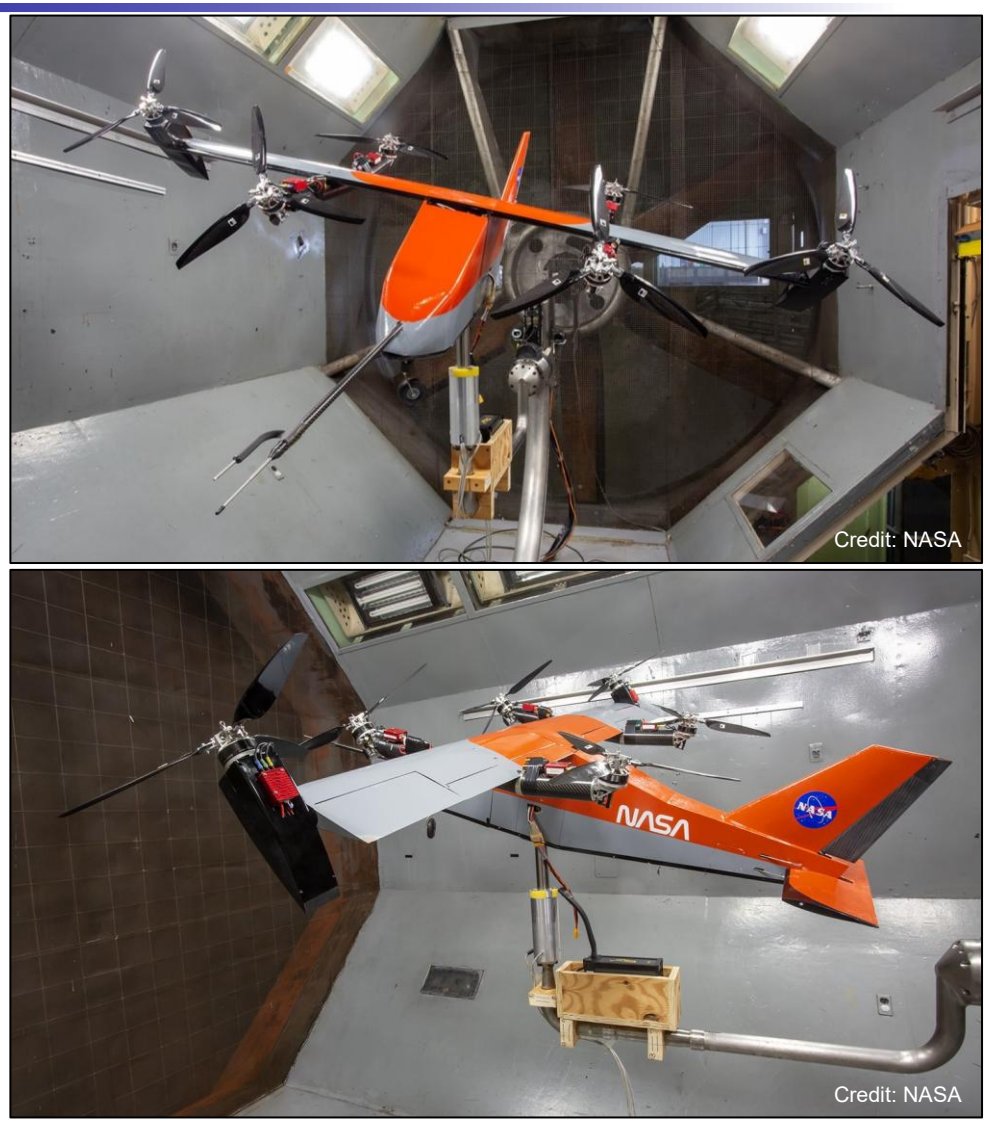
Modeling/validation normalized root-mean-square error (NRMSE) for each local model.

Dynamic Wind-Tunnel Testing

Simmons, B. M., Ackerman, K. A., and Asper, G. D., “Aeropropulsive Damping Characterization for eVTOL Aircraft Using Free-Motion Wind-Tunnel Testing,” *Journal of Aircraft*, Vol. 63, No. 2, 2026, pp. 465–479.

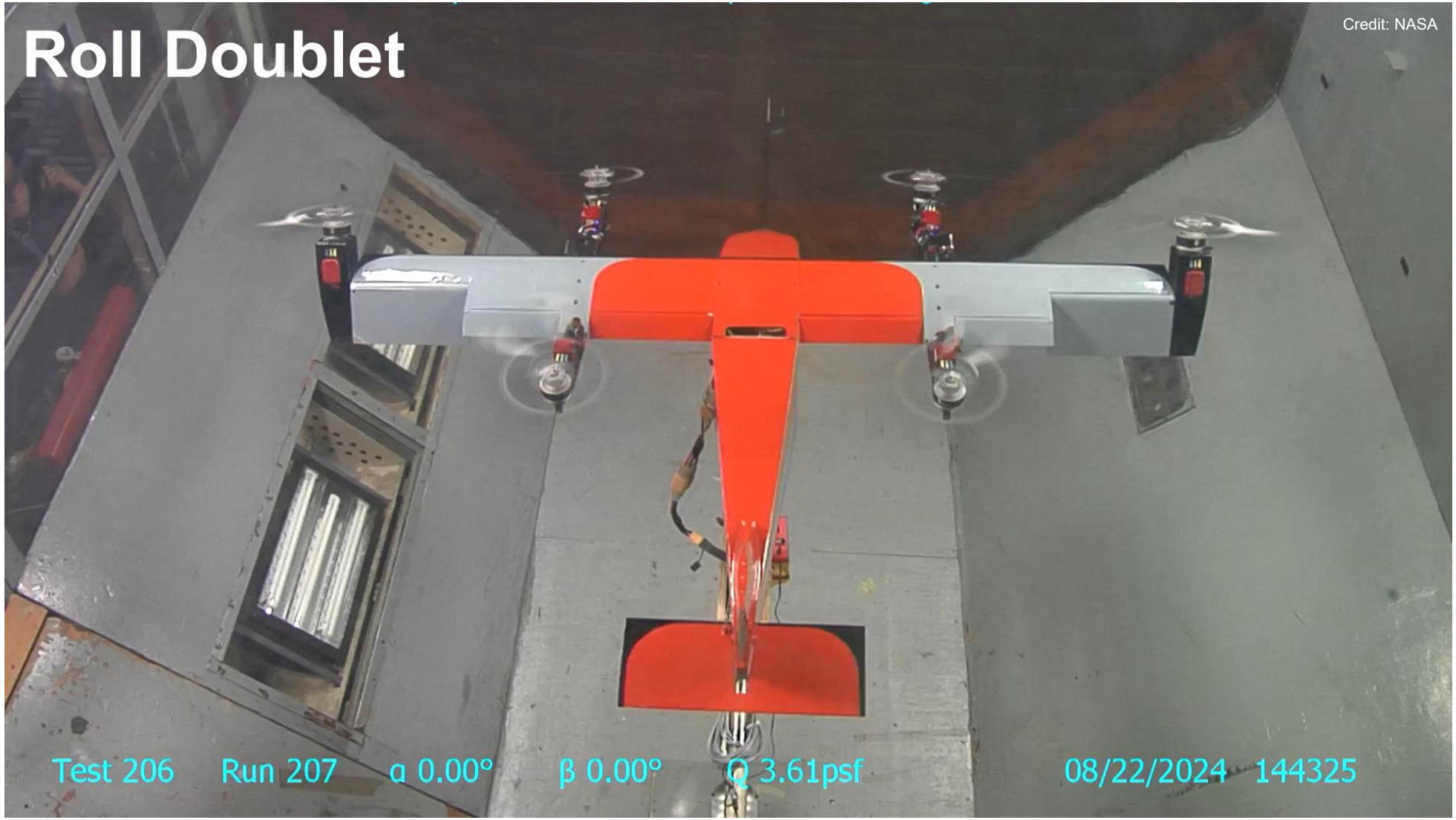
Three Degree-of-Freedom (3DOF) Testing

- New 3DOF rig designed and built in-house
  - Free rotational motion
  - Aerodynamic damping characterization
  - Flight control algorithm evaluation
- Custom RAVEN-SWFT 3DOF control system
  - Model-based control design approach
  - Tracks commanded attitude angles
  - Scheduling with dynamic pressure
  - Programmed test input (PTI) injection capability
  - Control algorithm deployed to an onboard Pixhawk
- Wind-tunnel testing approach
  - Dynamic pressure set using the wind-tunnel system
  - RC transmitter and GCS computer command vehicle
  - Onboard instrumentation – no balance
  - Similar hardware and software used for flight testing



RAVEN-SWFT mounted on a 3DOF rig.

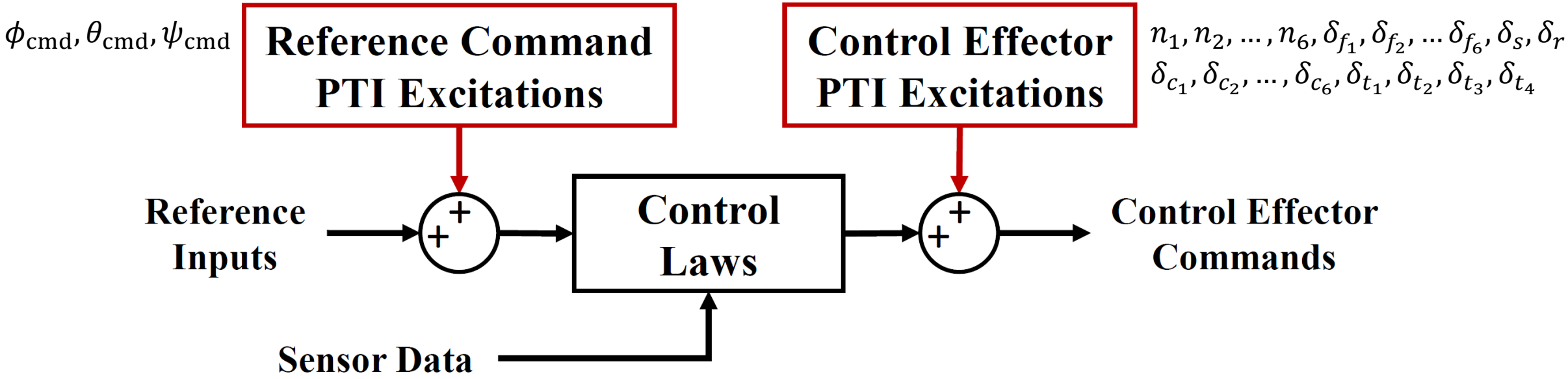
RAVEN-SWFT 3DOF Test Video



Attitude step commands at $\bar{q}$ = 3.79 lbf/ft^2.

Experiment Design Overview

- **Objective:** generate informative data for model identification
- Multiple-input excitation required for efficient testing → multisines
- Programmed test inputs (PTIs) integrated into flight control software
- Includes reference command and control effector PTI excitations



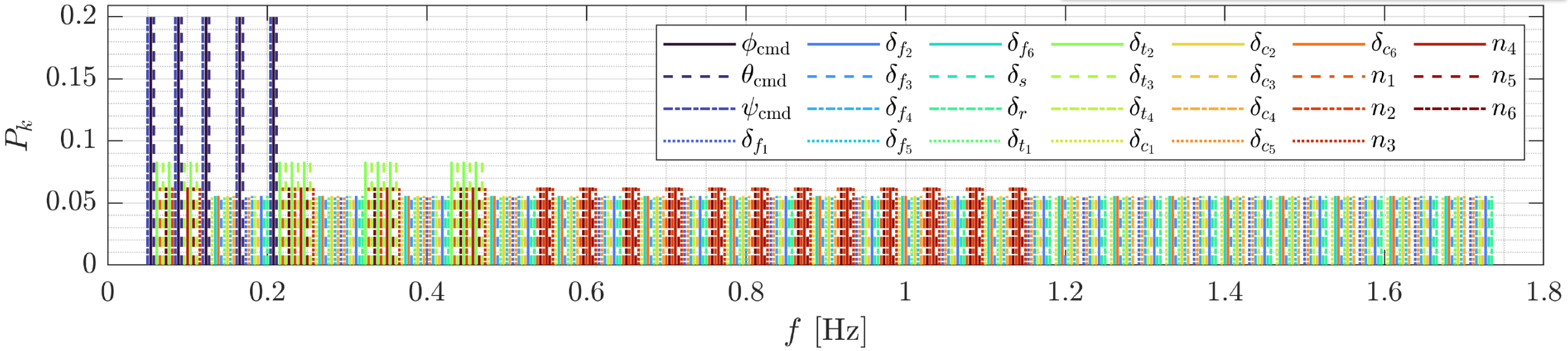
Programmed test input injections relative to the control laws.

3DOF Multisine Input Design

- Orthogonal phase-optimized multisine inputs[1,2]
- 27 unique multisine PTI excitation signals
- Simultaneous excitation in all axes

$$\boldsymbol{u_j} = \sum_{k \in K_j} A\sqrt{P_k} \sin\left(\frac{2\pi k \boldsymbol{t}}{T} + \phi_k\right)$$

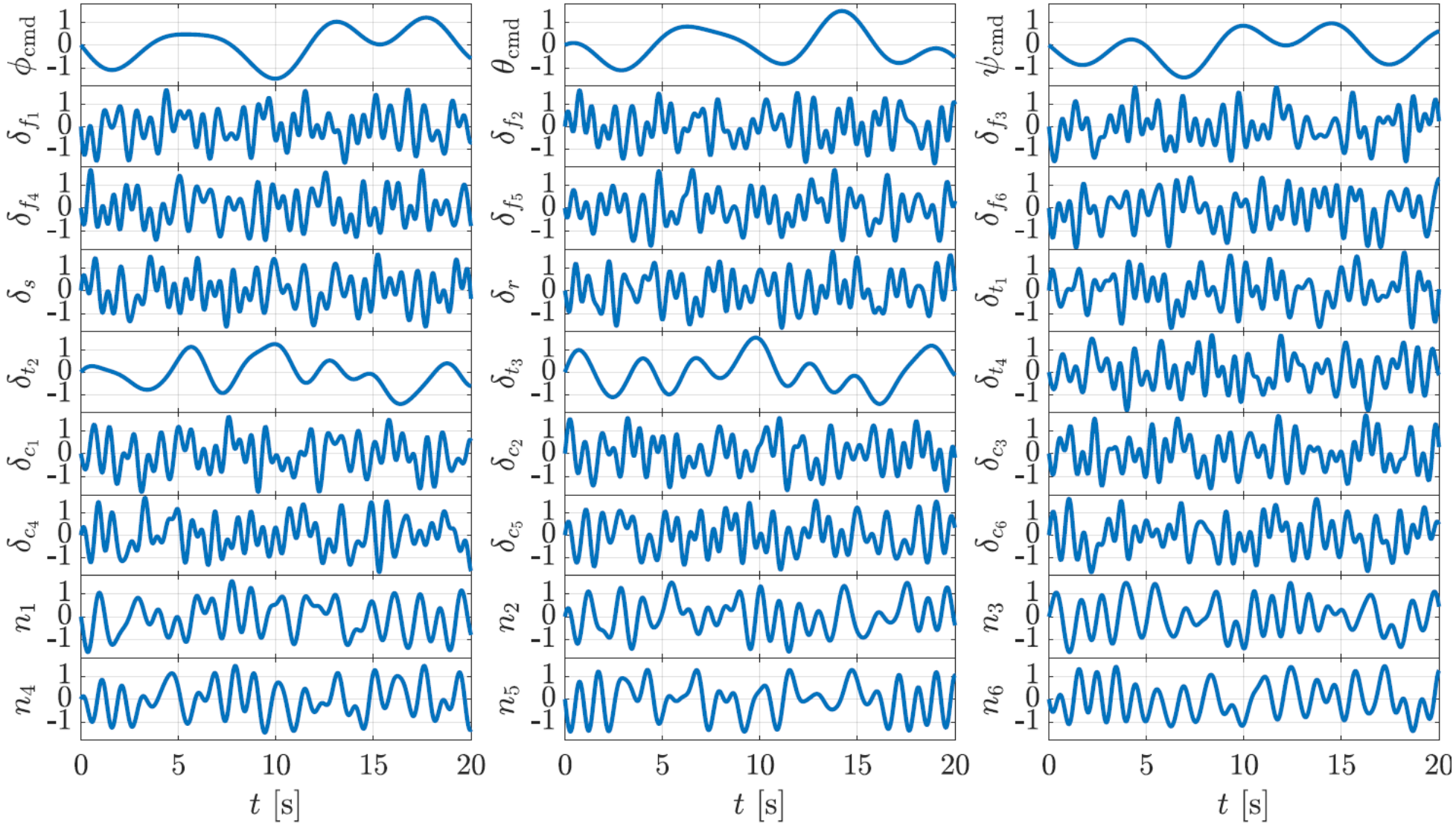
$\boldsymbol{u_j}$ – jth multisine signal
A – signal amplitude
P_k – kth power fraction
T – fundamental period
ϕ_k – kth phase angle



RAVEN-SWFT vehicle multisine input spectra.

1. Morelli, E. A., "Multiple Input Design for Real-Time Parameter Estimation in the Frequency Domain," *13th IFAC Conference on System Identification*, Aug. 2003.
2. Morelli, E. A., and Klein, V., *Aircraft System Identification: Theory and Practice*, 2nd ed., Sunflyte Enterprises, Williamsburg, VA, 2016.

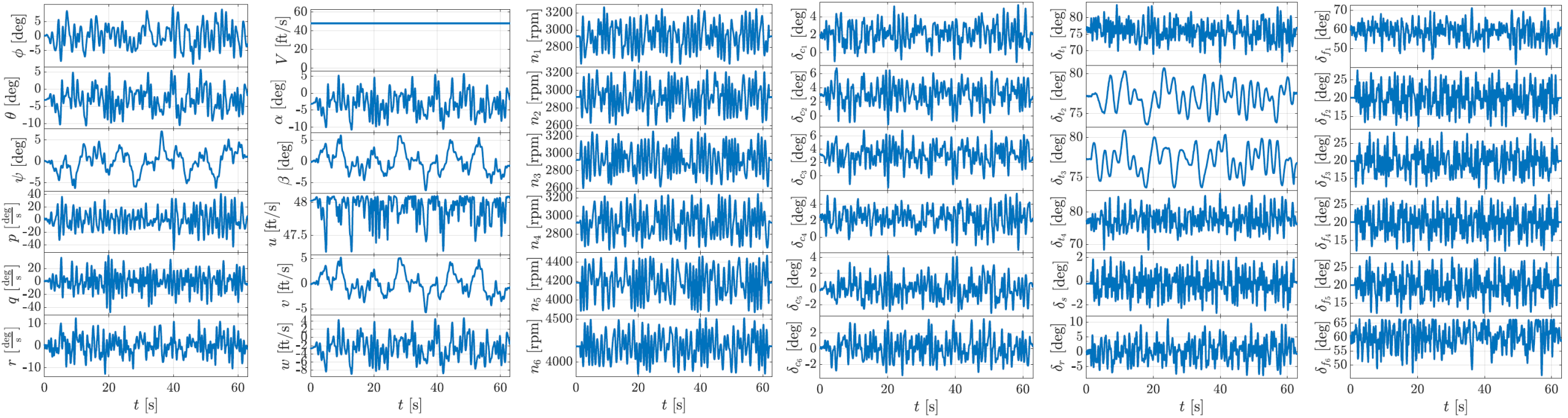
RAVEN-SWFT 3DOF Multisine Signals



RAVEN-SWFT normalized attitude and control effector multisine inputs.

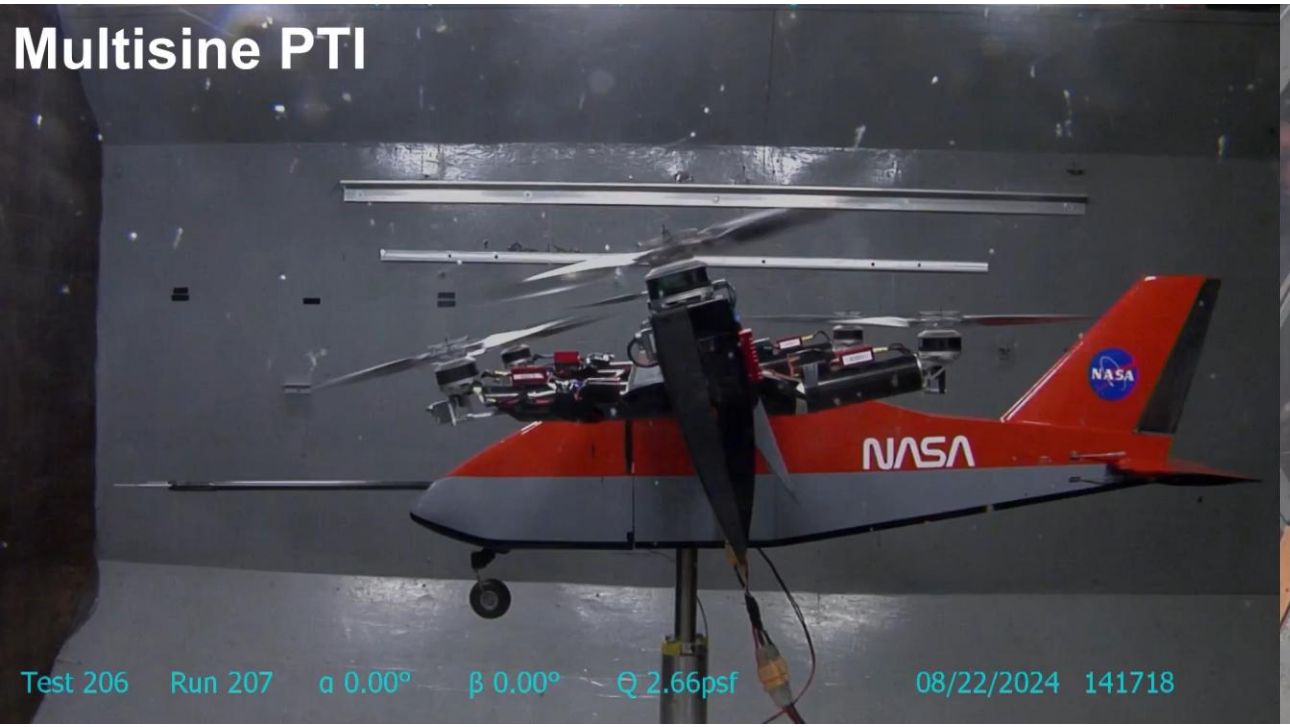
Example Maneuver ($\bar{q}$ = 2.75 lbf/ft^2)

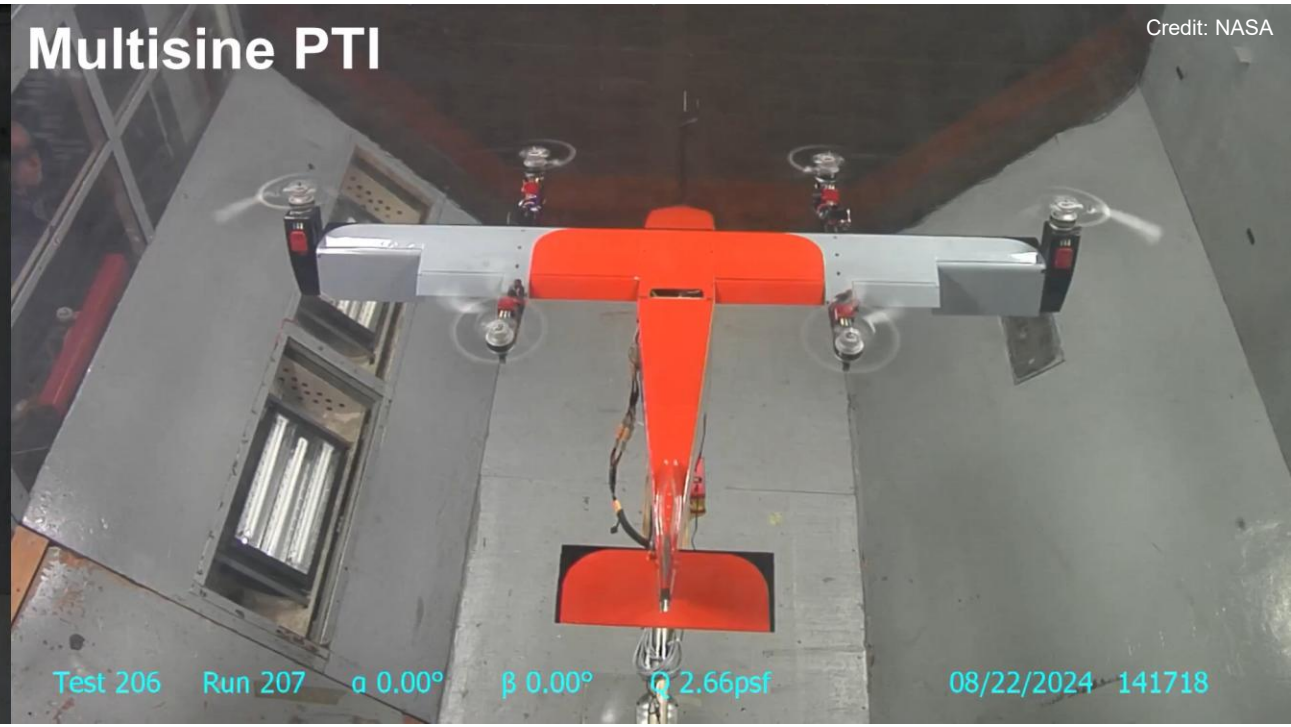
- Approximately 60-second multisine maneuvers executed for model ID
  - First ~50 seconds used for model identification
  - Last 10 seconds used for model validation
- Multiple multisine maneuvers were executed at each reference $\bar{q}$
- Data acquired with a single multisine maneuver are sufficient



RAVEN-SWFT 3DOF Multisine Maneuver

- PTIs are injected into the attitude and control effector commands
- All aircraft dynamics of interest are simultaneously excited
- Flight controller stabilizes the vehicle and tracks the commanded attitude





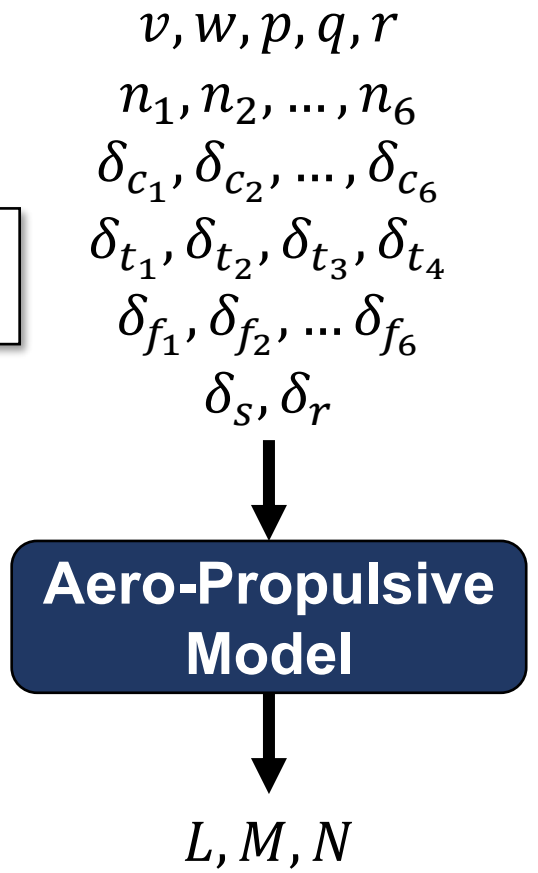
Multisine PTI excitations at $\bar{q}$ = 2.75 lbf/ft^2.

Model Identification Approach

- Aero-propulsive modeling framework tailored to eVTOL aircraft[1]
- Flight condition variable: dynamic pressure $\bar{q}$ (or freestream velocity V)
- Explanatory variables:
  - Body-axis velocity components (v, w)
  - Body-axis angular rates (p, q, r)
  - Proprotor rotational speeds $(n_1, n_2, \ldots, n_6)$
  - Control deflection angles $(\delta_{c_1}, \delta_{c_2}, \ldots, \delta_{c_6}, \delta_{t_1}, \delta_{t_2}, \delta_{t_3}, \delta_{t_4}, \delta_{f_1}, \delta_{f_2}, \ldots \delta_{f_6}, \delta_s, \delta_r)$

u effects are captured by models being developed at multiple $\bar{q}$ settings

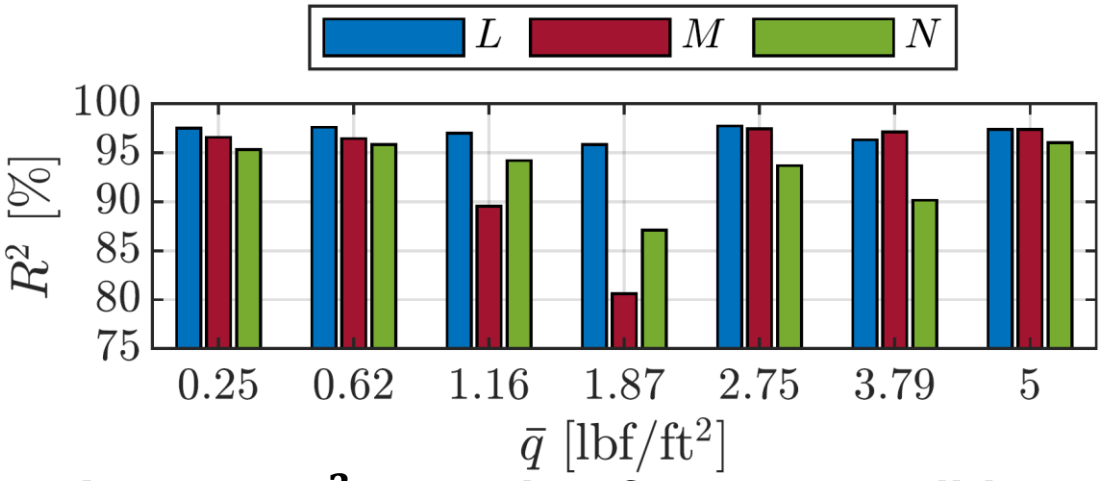
- Response variables:
  - Dimensional body-axis aero-propulsive moments (L, M, N)
  - Current study lacked instrumentation to measure applied forces (X, Y, Z)
- Nonlinear response surface equations (RSEs) developed at each $\bar{q}$
  - Model structure determination: stepwise regression
  - Parameter estimation: complex least-squares regression
  - Final weighted-mean parameter estimates computed from multiple maneuvers
- Damping parameters included at each condition: L_p, L_r, M_q, N_p, N_r ← **Main Deliverable**



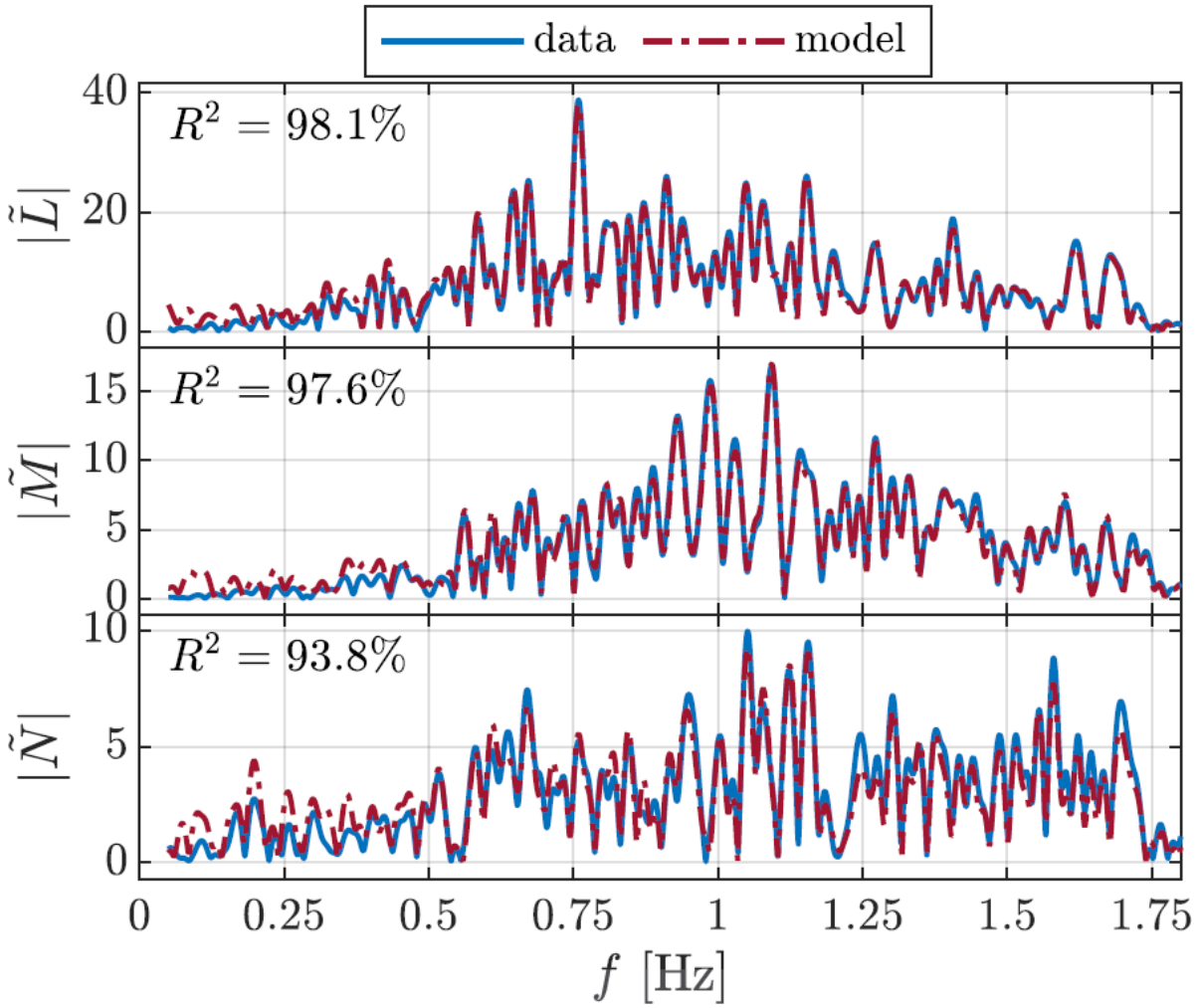
1. Simmons, B. M., and Murphy, P. C., "Aero-Propulsive Modeling for Tilt-Wing, Distributed Propulsion Aircraft Using Wind Tunnel Data," *Journal of Aircraft*, Vol. 59, No. 5, 2022, pp. 1162–1178.
2. Morelli, E. A., and Klein, V., Aircraft System Identification: Theory and Practice, 2nd ed., Sunflyte Enterprises, Williamsburg, VA, 2016.

Local Modeling Results ($\bar{q}$ = 2.75 lbf/ft²)

- Complex least-squares regression
- Good model fit
- High R^2 value
- Similar results obtained at each reference flight condition



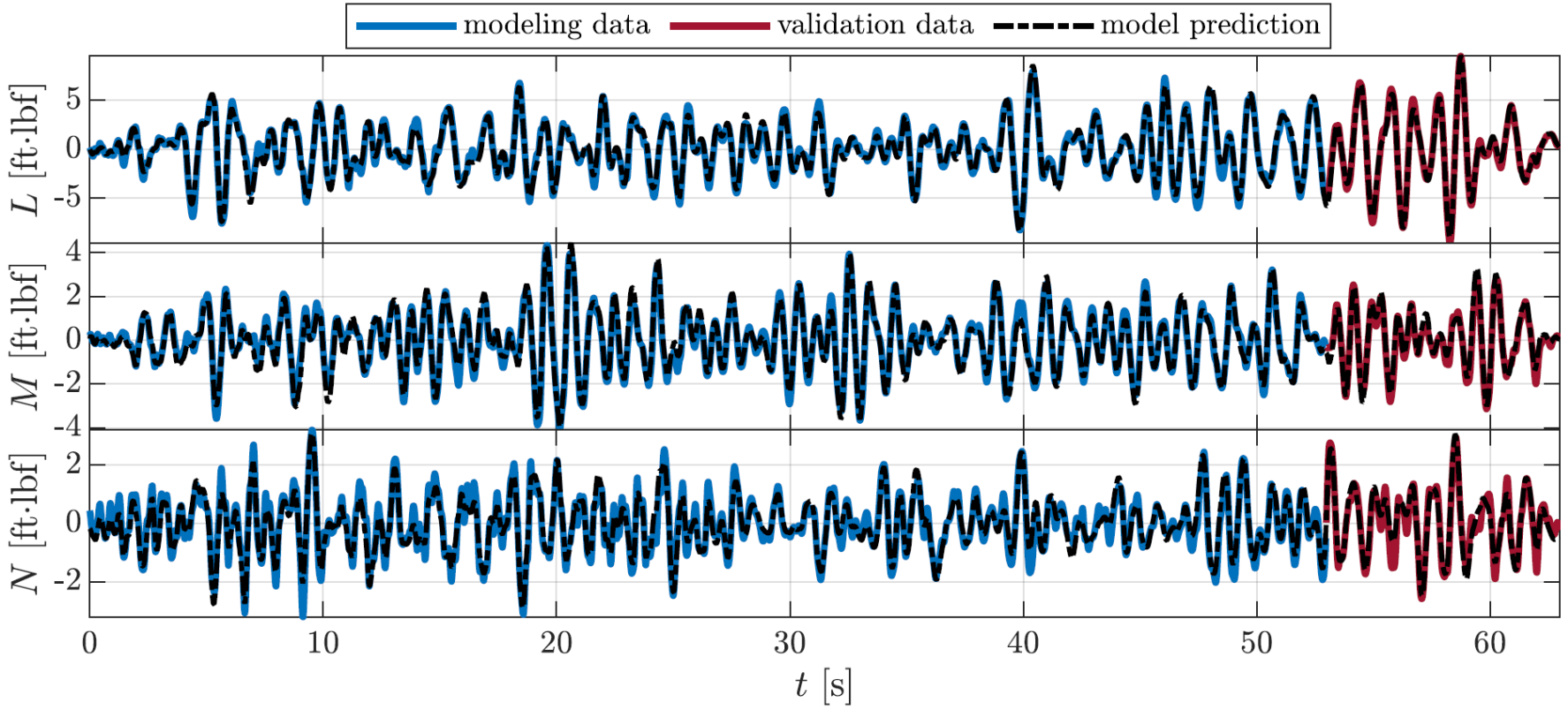
Average R^2 at each reference condition.



Comparison of modeling response data and model fit in the frequency domain.

Local Modeling Results ($\bar{q}$ = 2.75 lbf/ft^2)

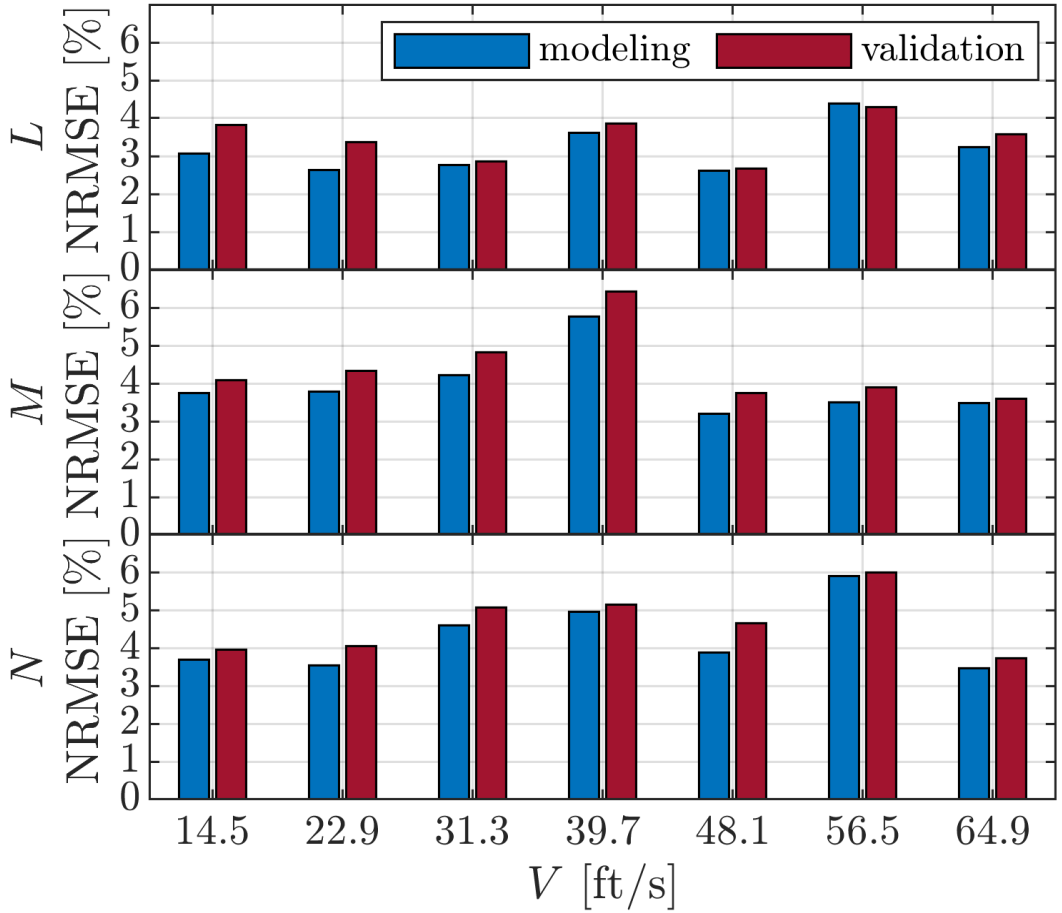
- Time-domain comparison of model prediction to smoothed responses
- Good prediction capability using weighted-mean parameter estimates
- Similar results for other flight conditions



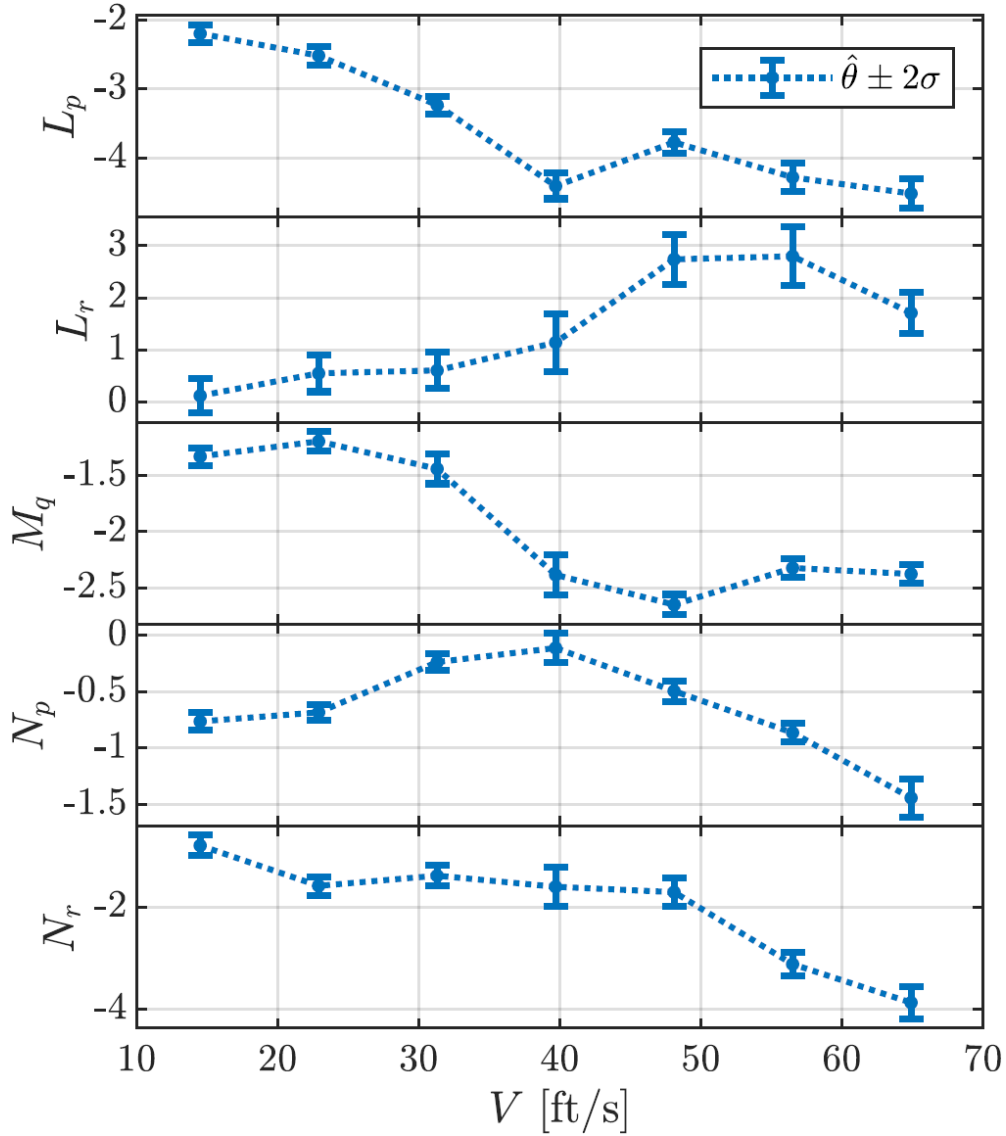
Comparison of time-domain response data and model prediction for a multisine maneuver.

Global Transition Modeling Results

$$\text{NRMSE} = 100 \times \frac{1}{\text{range}(\boldsymbol{z}_m)} \sqrt{\frac{(\boldsymbol{z}-\hat{\boldsymbol{y}})^T (\boldsymbol{z}-\hat{\boldsymbol{y}})}{N}}$$



Normalized root-mean-square error (NRMSE).



Dynamic derivative estimates.

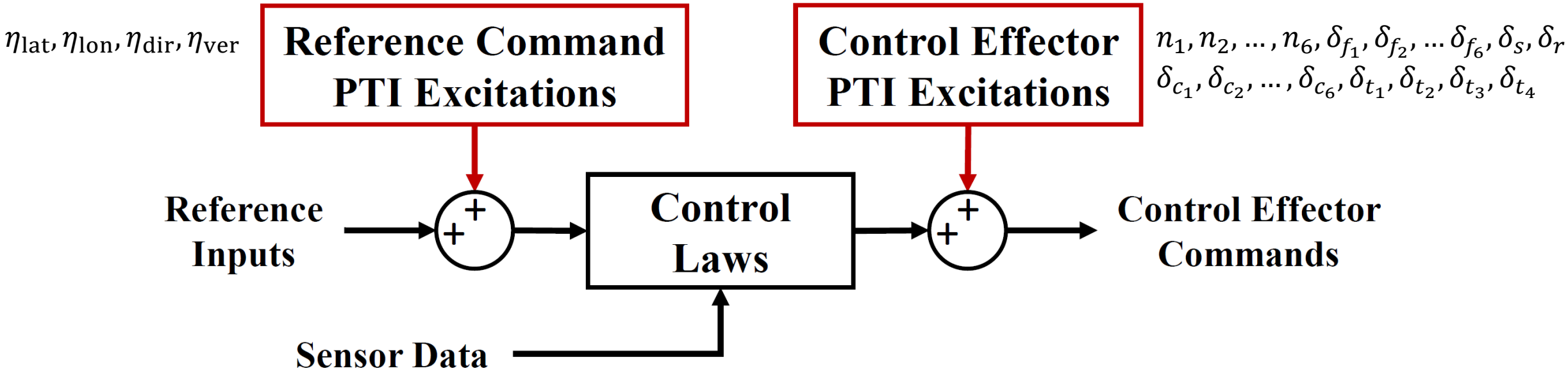
Flight-Test System ID

Simmons, B. M., and Ackerman, K. A., “System Identification for a Subscale Tiltrotor eVTOL Aircraft from Hover Flight-Test Data,” *AIAA SciTech Forum*, January 2026.

System Identification Approach

- Development of a mathematical model from flight-test data
- Present application: hover system ID
- Present motivation:
  - Demonstration of system ID approach
  - Improve vehicle aero-propulsive model

- Desired attributes:
  - Open-loop model identification
  - Efficient flight-test execution
  - Determine the independent effectiveness of all controls
  - Include nonlinear aerodynamics and control interaction effects



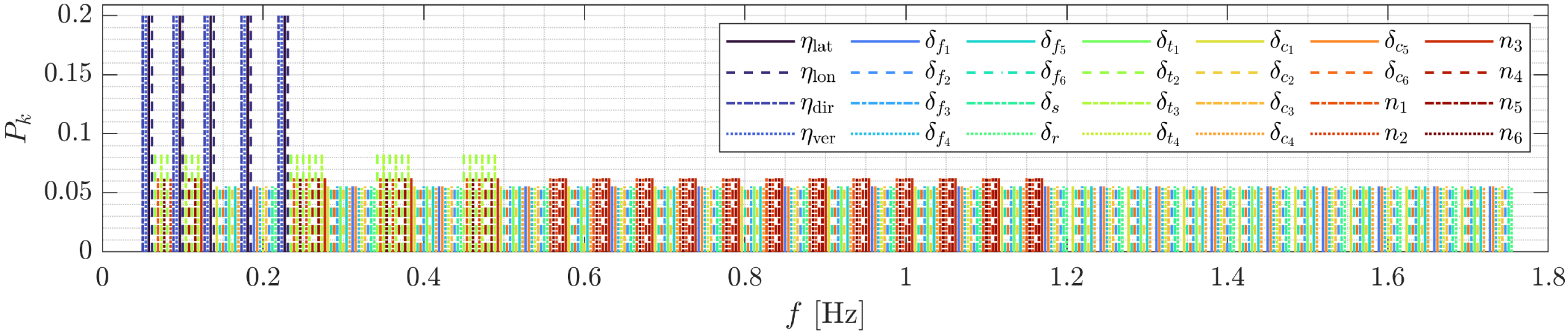
PTI injections relative to the control laws.

Flight-Test Multisine Input Design

- Orthogonal phase-optimized multisine inputs[1,2]
- 28 unique multisine PTI excitation signals
- Simultaneous excitation in all axes
- Reference command and control effector PTIs

$$u_j(t) = \sum_{k \in K_j} A\sqrt{P_k} \sin\left(\frac{2\pi k t}{T} + \phi_k\right)$$

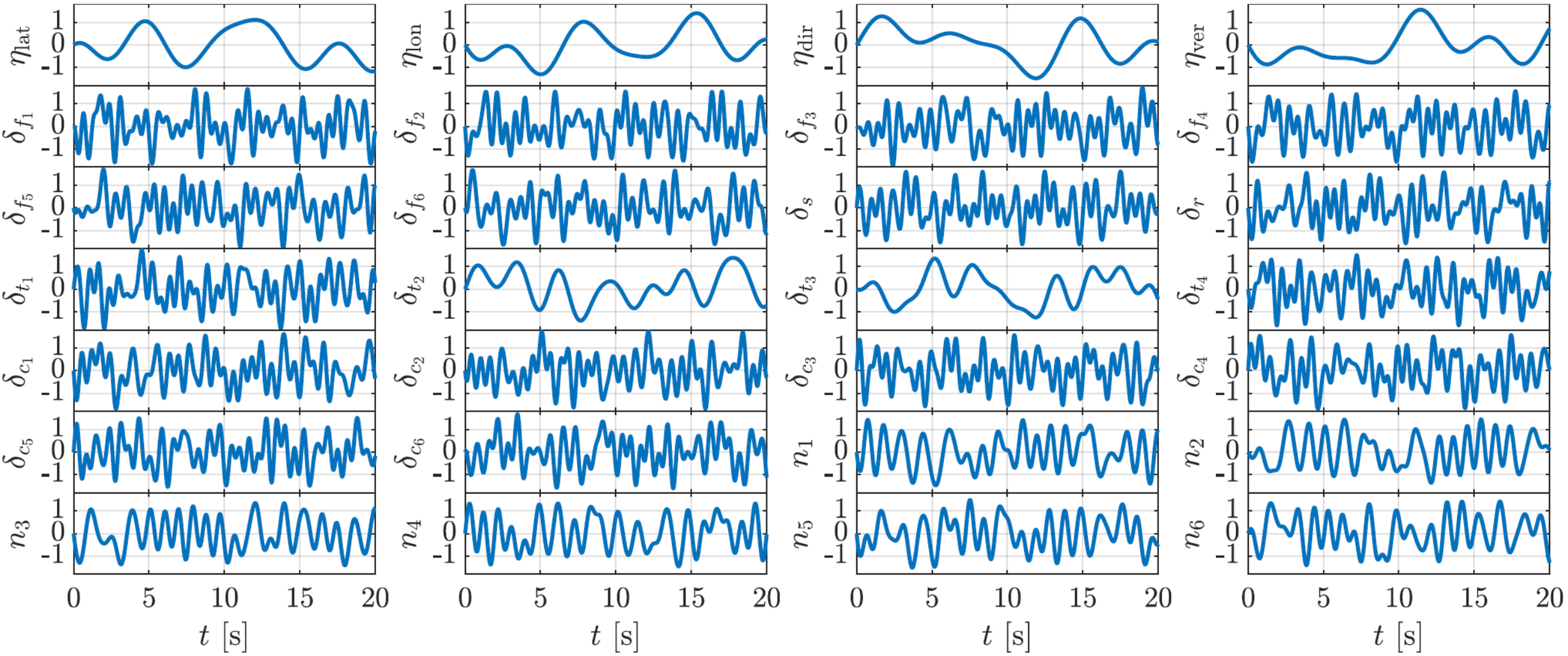
$u_j(t)$ – jth multisine signal
A – signal amplitude
P_k – kth power fraction
T – fundamental period
ϕ_k – kth phase angle



RAVEN-SWFT vehicle multisine input spectra.

1. Morelli, E. A., "Multiple Input Design for Real-Time Parameter Estimation in the Frequency Domain," *13th IFAC Conference on System Identification*, Aug. 2003.
2. Morelli, E. A., and Klein, V., *Aircraft System Identification: Theory and Practice*, 2nd ed., Sunflyte Enterprises, Williamsburg, VA, 2016.

RAVEN-SWFT Multisine Signals



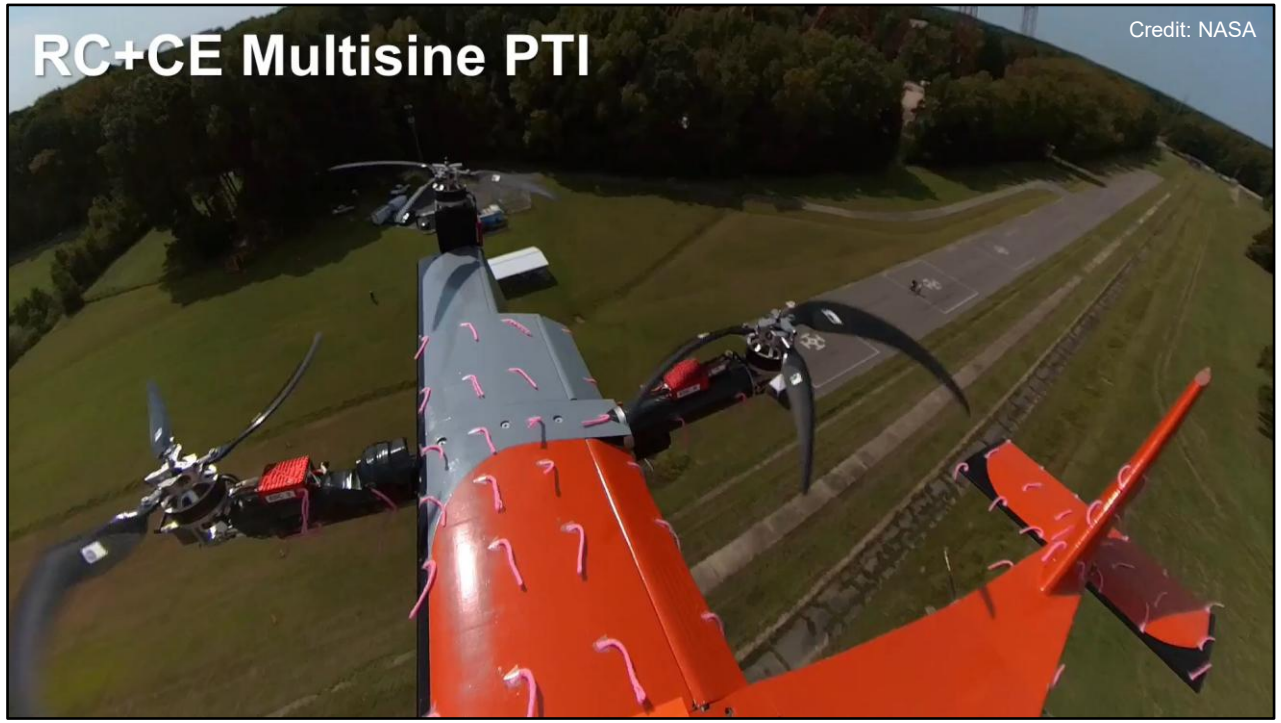
Normalized reference command and control effector multisine inputs.

Hover Flight-Test Maneuvers

- Multiple maneuvers were considered and studied for hover system ID
- Two maneuver types applying multisine inputs were preferred
  - Control effector (CE) multisine maneuver
  - Reference command and control effector (RC+CE) multisine maneuver



Hover CE multisine maneuver.



Hover RC+CE multisine maneuver.

Hover Maneuvers/Observations

CE = Control Effector
RC = Reference Command

CE multisine maneuver

- Larger control excitations
- Smaller u, v, w, r perturbations
- Improved control derivatives

RC+CE multisine maneuver

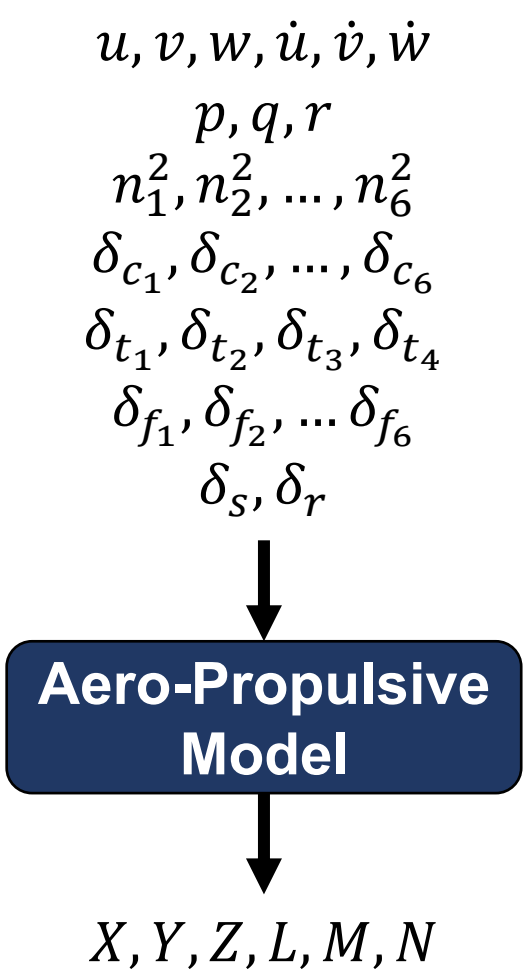
- Larger u, v, w, r perturbations
- Smaller control excitations
- Improved state derivatives





Model Identification Approach

- Aero-propulsive modeling framework tailored to eVTOL aircraft[1,2]
- Flight condition variable: airspeed (V)
- Explanatory variables:
  - Body-axis translational velocity components (u, v, w) and derivatives ($\dot{u}, \dot{v}, \dot{w}$)
  - Body-axis angular velocity components (p, q, r)
  - Squared proprotor rotational speeds[3] ($n_1^2, n_2^2, \ldots, n_6^2$) → Linear thrust changes $T = \rho n^2 D^4 C_T$
  - Control deflection angles ($\delta_{c_1}, \delta_{c_2}, \ldots, \delta_{c_6}, \delta_{t_1}, \delta_{t_2}, \delta_{t_3}, \delta_{t_4}, \delta_{f_1}, \delta_{f_2}, \ldots \delta_{f_6}, \delta_s, \delta_r$)
- Response variables (inferred from other measurements):
  - Dimensional body-axis aero-propulsive forces (X, Y, Z)
  - Dimensional body-axis aero-propulsive moments (L, M, N)
- Response surface equations (RSEs) developed at each condition
  - Model structure determination: combination of multivariate orthogonal function modeling (MOF)[3] and stepwise regression (SWR)[4]
  - Parameter estimation: complex least-squares regression[4]
  - Final parameter estimates computed using multiple maneuvers



1. Simmons, B. M., and Murphy, P. C., "Aero-Propulsive Modeling for Tilt-Wing, Distributed Propulsion Aircraft Using Wind Tunnel Data," *Journal of Aircraft*, Vol. 59, No. 5, 2022, pp. 1162–1178.
2. Simmons, B. M., "System Identification Approach for eVTOL Aircraft Demonstrated Using Simulated Flight Data," *Journal of Aircraft*, Vol. 60, No. 4, 2023, pp. 1078–1093.
3. Simmons, B. M., Rapsomanikis, A., Jacobellis, G., Ofodile, N., Hamilton, T., and Ma, M., "Flight-Test System Identification Methodology and Hover Results for a Vectored-Thrust eVTOL Aircraft," *VFS Annual Forum*, May 2025.
4. Morelli, E. A., and Klein, V., *Aircraft System Identification: Theory and Practice*, 2nd ed., Sunflyte Enterprises, Williamsburg, VA, 2016.

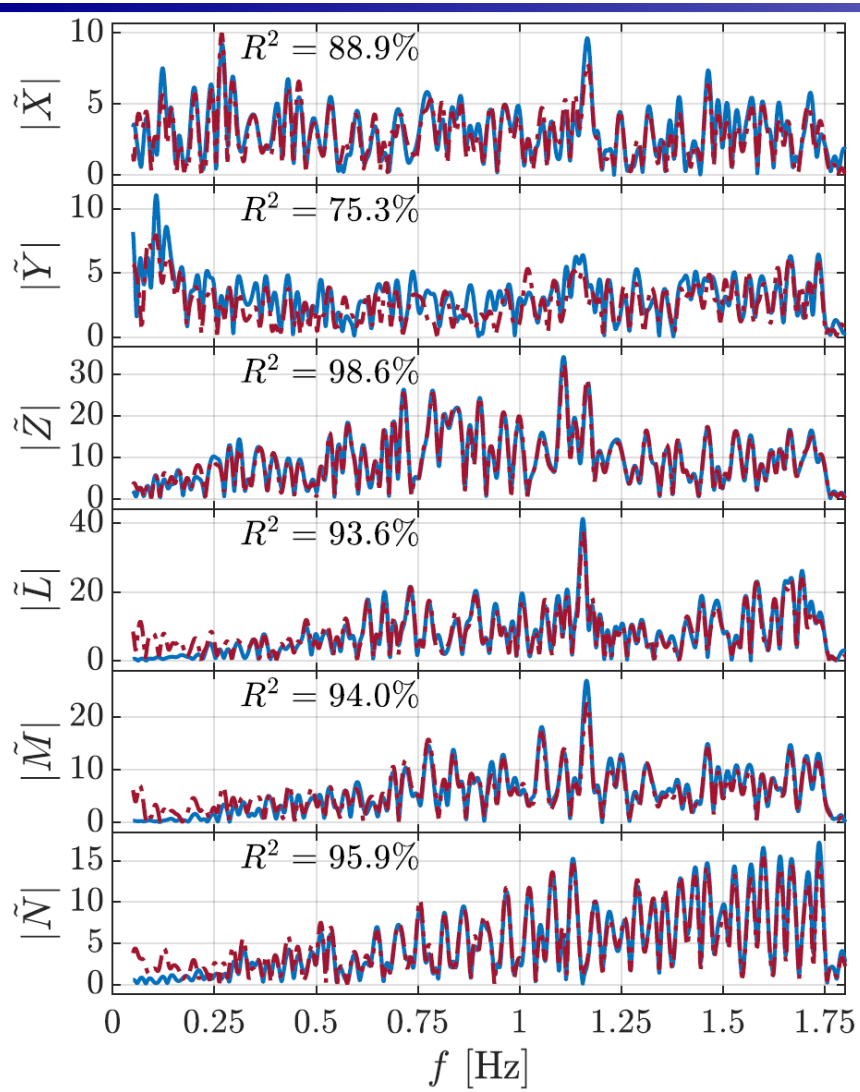
Hover Model Structure

- Nonlinear terms considered/included
- Model parameter symmetrization

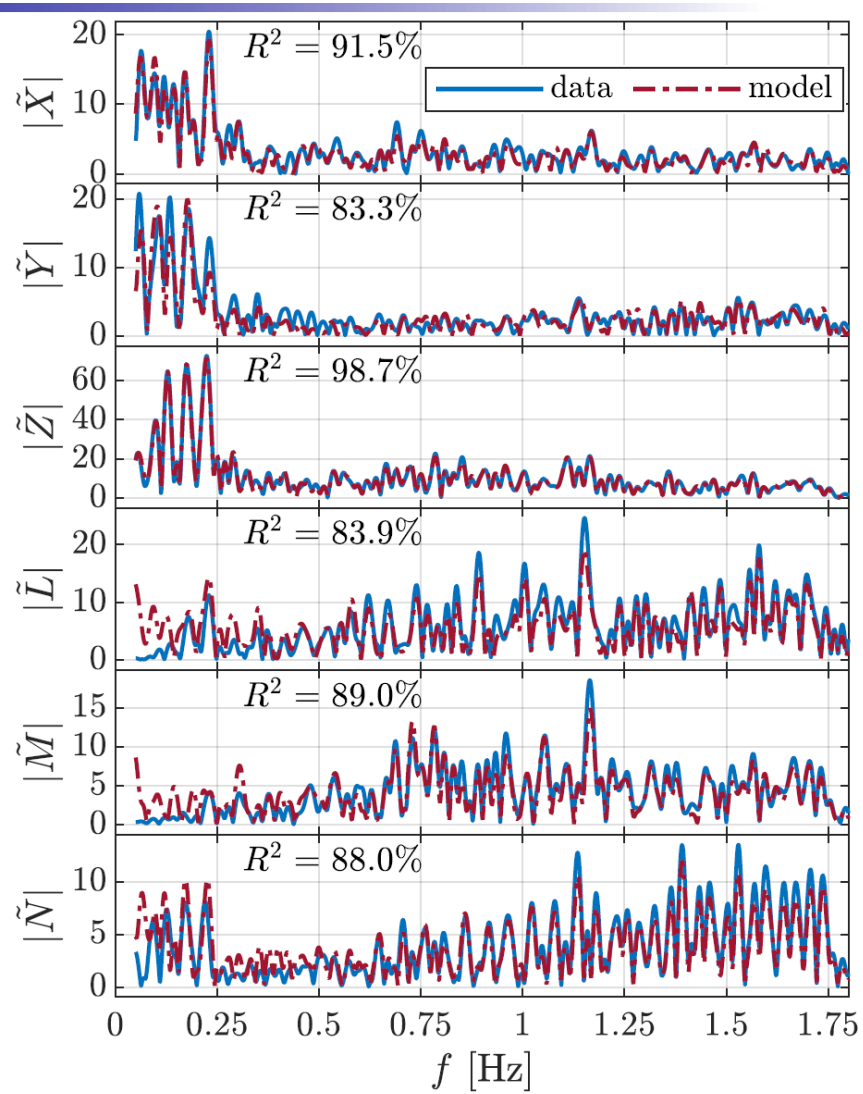
$$
\begin{aligned}
X &= X_u u + X_w w + X_{wq} wq + X_{\delta_{f16}}(\delta_{f_1} + \delta_{f_6}) + X_{\delta_{t14}}(\delta_{t_1} + \delta_{t_4}) + X_{\delta_{t23}}(\delta_{t_2} + \delta_{t_3}) + X_{\delta_{c23}}(\delta_{c_2} + \delta_{c_3}) \\
&\quad + X_{\delta_{c56}}(\delta_{c_5} + \delta_{c_6}) + X_{n_{23}^2}(n_2^2 + n_3^2) + X_{n_{56}^2}(n_5^2 + n_6^2) + X_{n_{14}^2\delta_{t14}}(n_1^2\delta_{t_1} + n_4^2\delta_{t_4}) + X_{n_{23}^2\delta_{t23}}(n_2^2\delta_{t_2} + n_3^2\delta_{t_3}) \\
&\quad + X_{\delta_{c14}\delta_{t14}}(\delta_{c_1}\delta_{t_1} + \delta_{c_4}\delta_{t_4}) + X_{\delta_{c23}\delta_{t23}}(\delta_{c_2}\delta_{t_2} + \delta_{c_3}\delta_{t_3}) + X_o \\
Y &= Y_v v + Y_{\delta_{t14}}(\delta_{t_1} - \delta_{t_4}) + Y_{\delta_{t23}}(\delta_{t_2} - \delta_{t_3}) + Y_{\delta_{c14}}(\delta_{c_1} - \delta_{c_4}) + Y_{\delta_{c23}}(\delta_{c_2} - \delta_{c_3}) + Y_{\delta_{c56}}(\delta_{c_5} - \delta_{c_6}) \\
&\quad + Y_{n_{14}^2}(n_1^2 - n_4^2) + Y_{n_{23}^2}(n_2^2 - n_3^2) + Y_{n_{56}^2}(n_5^2 - n_6^2) \\
Z &= Z_w w + Z_{uq} uq + Z_{vp} vp + Z_{\dot{w}} \dot{w} + Z_{\delta_{c14}}(\delta_{c_1} + \delta_{c_4}) + Z_{\delta_{c23}}(\delta_{c_2} + \delta_{c_3}) + Z_{\delta_{c56}}(\delta_{c_5} + \delta_{c_6}) + Z_{n_{14}^2}(n_1^2 + n_4^2) \\
&\quad + Z_{n_{23}^2}(n_2^2 + n_3^2) + Z_{n_{56}^2}(n_5^2 + n_6^2) + Z_o \\
L &= L_v v + L_p p + L_{wr} wr + L_{vr} vr + L_{\delta_{f16}}(\delta_{f_1} - \delta_{f_6}) + L_{\delta_{t14}}(\delta_{t_1} - \delta_{t_4}) + L_{\delta_{c14}}(\delta_{c_1} - \delta_{c_4}) + L_{\delta_{c23}}(\delta_{c_2} - \delta_{c_3}) \\
&\quad + L_{\delta_{c56}}(\delta_{c_5} - \delta_{c_6}) + L_{n_{14}^2}(n_1^2 - n_4^2) + L_{n_{23}^2}(n_2^2 - n_3^2) + L_{n_{56}^2}(n_5^2 - n_6^2) \\
M &= M_u u + M_w w + M_{uq} uq + M_{wq} wq + M_{vp} vp + M_{\dot{w}} \dot{w} + M_{\delta_{c23}}(\delta_{c_2} + \delta_{c_3}) + M_{\delta_{c56}}(\delta_{c_5} + \delta_{c_6}) \\
&\quad + M_{n_{23}^2}(n_2^2 + n_3^2) + M_{n_{56}^2}(n_5^2 + n_6^2) + M_o \\
N &= N_r r + N_{\delta_{f16}}(\delta_{f_1} - \delta_{f_6}) + N_{\delta_{t14}}(\delta_{t_1} - \delta_{t_4}) + N_{\delta_{t23}}(\delta_{t_2} - \delta_{t_3}) + N_{\delta_{c14}}(\delta_{c_1} - \delta_{c_4}) + N_{\delta_{c23}}(\delta_{c_2} - \delta_{c_3}) \\
&\quad + N_{n_{14}^2}(n_1^2 - n_4^2) + N_{n_{23}^2}(n_2^2 - n_3^2) + N_{n_{14}^2\delta_{t14}}(n_1^2\delta_{t_1} - n_4^2\delta_{t_4}) + N_{\delta_{c14}\delta_{t14}}(\delta_{c_1}\delta_{t_1} - \delta_{c_4}\delta_{t_4}) + I_p(\textstyle\sum_{i=1}^{6}(-1)^i\dot{\Omega}_i)
\end{aligned}
$$

Frequency-Domain Hover Modeling Results

- Complex least-squares regression
- Maneuvers first analyzed separately
- Good overall fits
- Similar results for repeated maneuvers



CE multisine maneuver

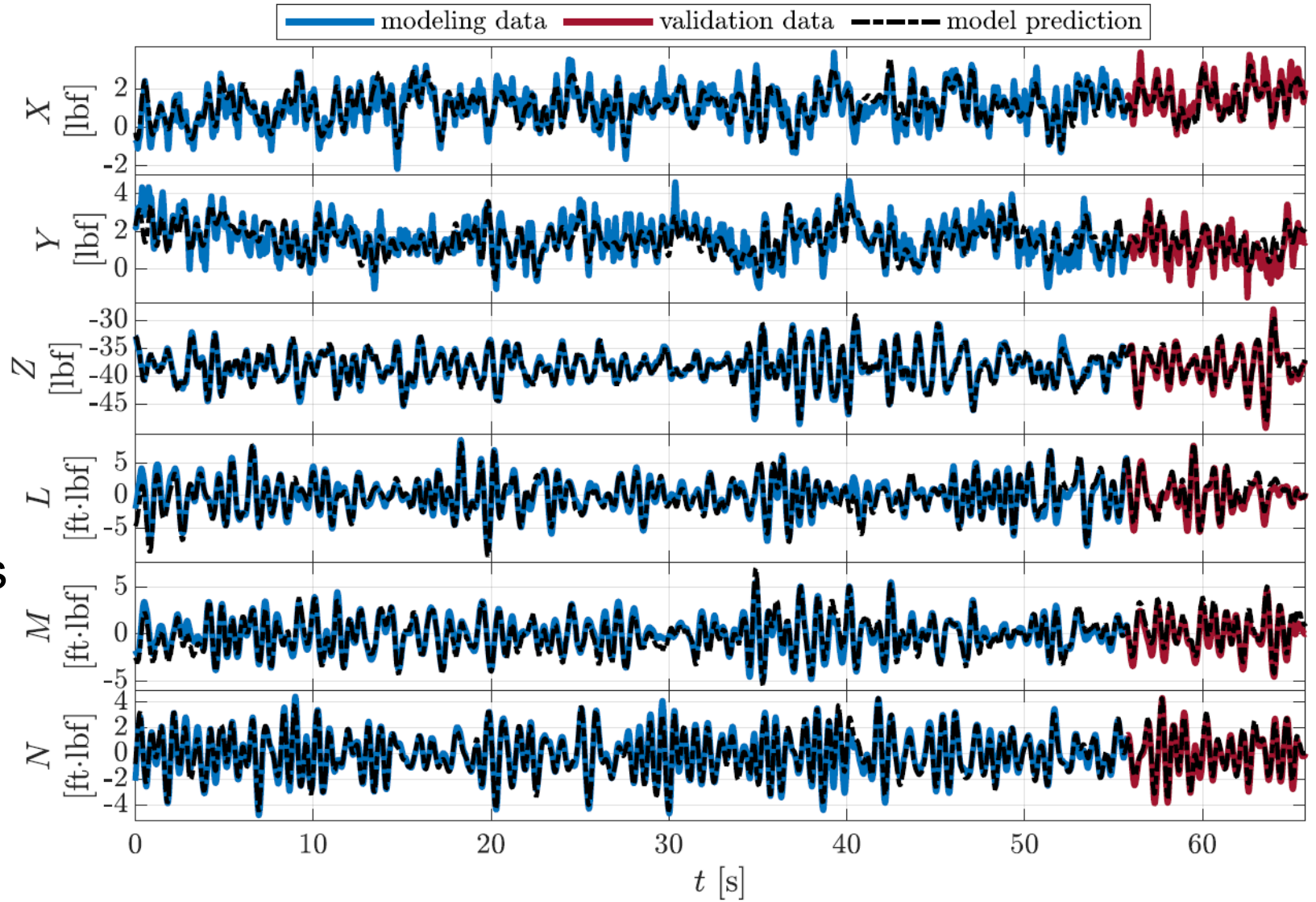


RC+CE multisine maneuver

Comparison of response data and model fit for example maneuvers.

Hover Model Prediction: CE Multisine

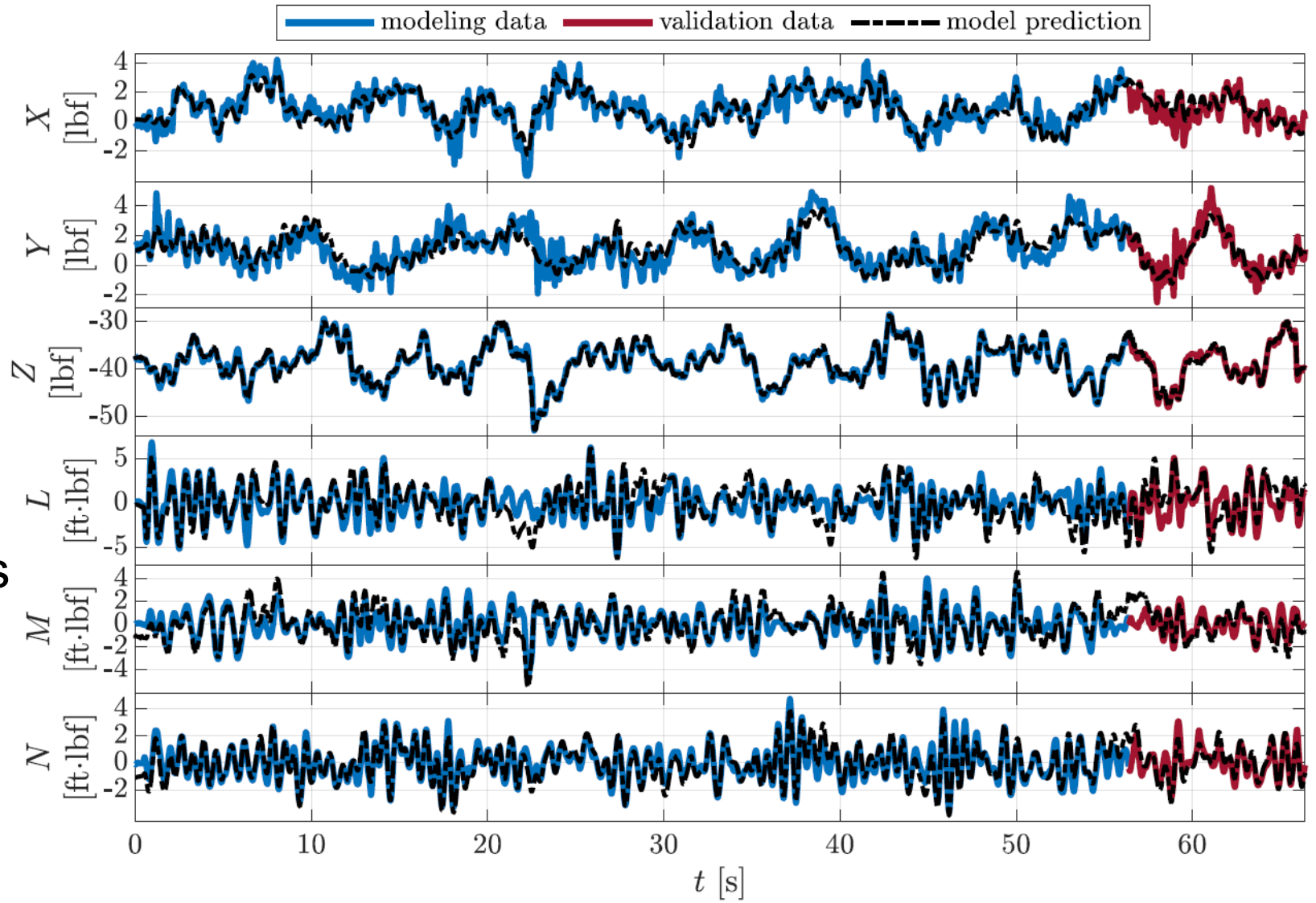
- Time-domain comparison of model prediction to smoothed response data
- Last 10 seconds of each maneuver withheld for model validation
- Good prediction capability using combined parameters



Comparison of response data and model prediction.

Hover Model Prediction: RC+CE Multisine

- Time-domain comparison of model prediction to smoothed response data
- Last 10 seconds of each maneuver withheld for model validation
- Good prediction capability using combined parameters



Comparison of response data and model prediction.

Conclusions and Next Steps

Concluding Remarks

- eVTOL aircraft present new aero-propulsive modeling challenges
- Efficient test execution employing DOE/RSM and multisine inputs
- PTI injections before and after the control laws are important for 3DOF/flight
- Accurate aero-propulsive models created from wind-tunnel and flight testing
- Techniques can be applied throughout transition and for many vehicles
- Significant progress in modeling approaches for complex aircraft





Next Steps

- Flight-test system identification in transition and forward flight
- NASA RAVEN 1000-lb-class vehicle[1]
  - Research platform providing open geometry, data, and methods
  - Tiltrotor configuration relevant to eVTOL vehicles being developed in industry
  - Initial research emphasis on aero-propulsive characterization, flight controls, and acoustics
- Active research is further refining eVTOL vehicle modeling and control techniques
- Open to establishing additional collaboration opportunities

1. https://www.nasa.gov/raven/



NASA RAVEN vehicle renderings.

Ward Lecture Acknowledgements



- Gene Morelli
- Corey Diebler
- Oscar Murillo
- Colleagues
- Marge Draper-Donley
- John Valasek
- ACGSC Planning and Advisory Board
- Dave Ward Memorial Lecture Selection Committee

Acknowledgment of NASA Team

- **Funding:** NASA Transformational Tools and Technologies (TTT) and Flight Demonstrations and Capabilities (FDC) projects
- **Flight controls:** Kasey Ackerman, Garrett Asper, Rachel Axten, and Steve Snyder
- **Vehicle development and flight testing:** Matthew Gray, Gregory Howland, Ryan Chan, David North, Steven Geuther, Justin Lisee, and Gary Banziger
- **RAVEN-SWFT pilots:** Jody Miller and Brayden Chamberlain
- **Wind-tunnel testing:** Ron Busan, Stephen Farrell, Earl Harris, Rick Thorpe, Clinton Duncan, Wes O'Neal, Lee Pollard, and Vincent Spada
- **Project leadership:** Siena Whiteside, Jason Welstead, Jake Schaefer, Steve Riddick, and Mike Acheson
- Recently expanded NASA RAVEN team

Questions/Discussion

Thank you for attending.



